Ben-Gurion University of the Negev
Department of Mechanical Engineering

Ph.D. Research Proposal
- Revised -

Grasping of Deformable Objects

By: Alon Ohev - Zion
Supervisors: Dr. Amir Shapiro

February 2011

Alon Ohev - Zion:	_____	Date:	October 17, 2011
Dr. Amir Shapiro:	_____	Date:	October 17, 2011
Prof. Avraham Levi :	_____	Date:	_____

Table of Contents

List of Figures

CHAPTER 1

Introduction

Grasping mechanisms (*grippers*) are used for a wide range of applications including fixturing arrangements, industrial, agricultural, and services robotics for medical and home use. The gripper must immobilize the object it is manipulating, while applying the minimal necessary gripper effort, in order to prevent the grasped object's bruising or the gripper being overly strenuous. This requires development of a grasp model.

The grasp model includes kinematic, dynamic and contact models [**112**]. The kinematic model defines the system's mechanical constraints [**118**], the dynamic model defines the dynamic reactions of the system's elements [**118**], and the contact model defines the coupling between the force and torque reactions between the object and the gripper to their deformations [**136**].

All grasp models are greatly dependent on the system's parameters, such as the number of contact points, the object's geometry, the gripper's structure, the desired object's manipulation, and the mechanical properties of the object and gripper [**79, 138, 98, 140**]. Some of the parameters are easier to define, such as the object's desired manipulation or the geometries of the object and the gripper. Other parameters, like the object's and the fingertip's mechanical properties and an appropriate contact model, are more difficult to define [**25, 27**].

Many contact models were developed in order to assess the reactions. They vary from considering rigid components and point fingertips with no friction at the contact point [**140, 96, 137**], to soft finger models – assuming elasticity or compliant components, which imply a contact surface with a spatial and distributed force and torque [**81, 127, 30, 136, 139**]. Note that the location of contact is referred to as "contact point", although geometrically it is a surface in some of the discussed models.

This work focuses on analyzing the object's geometry and the defined contact points in order to provide the set of forces and torques that can be applied to the grasped object, without losing its grasp. Grasp synthesis and grasp planning, are usually performed as a search in the system's configuration space, which is constrained by the selection of a specific gripper [**42, 43**]. The search process maps the configuration space, and assesses the grasp quality at each point, by the defined grasping quality criteria [**79, 43**]. This work presents a different approach. Instead of constraining a specific gripper, the external set forces and torques that can be applied to the object are determined; the synthesis will provide an optimal set of positions for n contact points. These positions will be optimal in the sense of minimal force and torque reactions at each contact point.

An important application of this work is for grasping fruits and vegetables. Agricultural produce are characterized by great shape diversity and usually fragile structure. These impose difficulties in grasping and gripper design, where it is desired to manipulate the object while preventing its bruising. Current state-of-the-art agricultural robotic grippers are specifically designed to match one specific product, e.g., eggplants [**44**], cucumbers [**28**], melons [**77**], watermelons [**105, 106**], strawberries [**22**], tomatoes [**76**], and general industrial food products [**107**]. These designs consider the stability and

the object's damage and bruising for a specific grasp's posture. These design process lacks systematic optimization of the grasp posture, and its effect on applied grasping forces.

1.1. Research Objectives

The main research objective of this work is to develop an optimal grasp synthesis tool. The specific objectives are to define the locations of a given number of contact points that provide:

1. A stable and firm grasp when applying the minimal grasping force.
2. A grasp with a maximal stability basin of attraction.

As an outcome of the performed synthesis, a gripper that will provide the desired grasping locations and grasping forces, can be designed.

1.2. Research Contribution and Innovations

The main research contributions include:

- **Spatial compliant grasp model.** Based on a compliant contact model [**30, 139**], a spatial grasp model will be derived, and its stability will be analyzed. This model will be an improvement to the current planar model in [**112, 98, 114**], and will further constitute the basis for the synthesis.
- **Optimal grasp synthesis.** Grasp synthesis and planning will include a search for an appropriate grasp in the multi-dimensional grasp-parameters space. In order to reduce the searchable space, the grasp parameters are usually coupled and bounded by the selection of a specific gripper and the approximation of the object [**80, 43**]. In this thesis, a synthesis that is independent of a specific gripper will be developed. The above will be achieved by matching a set of objects, loaded with a set of forces and torques, with a set of contact points that will provide the optimal grasp, based on the compliant grasp model and the optimization criterion.
- **Agricultural implementation.** This work will be the first to provide a grasp synthesis methodology, for optimal agricultural produce grasping. This will be specifically applied to sweet pepper and apple harvesting.

The core of this work will be achieved by performing recursion search in the grasp configuration parameter space, following the defined: fingertips and grasped object's geometry and mechanical properties, the set of external loads that can be applied to the object, and the number of grasping contact points. This search will be based on an optimization criterion, which will further provide a means to assess the quality of the statically indeterminate grasp's dynamic equations. The process is illustrated in Figure 3.1, and analytically defined by (3.4).

An important future extension of this work is the implementation of these contact points and desired grasping forces as gripper design objectives.

CHAPTER 2

Literature Review

This chapter reviews the ideas, innovations, concepts, problems, and solutions regarding grasp synthesis and planning with an orientation to foods and agricultural products. First, in section 2.1, the variety of agriculture and food processing robots are presented, with the description of different harvesting methods, which is followed by a vast survey of robotic grippers. Grasp models are presented in section 2.2, based on the major contact models. Organic matter's models, analysis, and measurements are reviewed as well. Analysis of the grasp and its stability are defined and described in section 2.3, which is followed by the grasp synthesis and planning 2.4. Finally in section 2.5, the computer simulations and the performed experiments are detailed.

2.1. Automation, Robotics, and Grippers

Robots are commonly utilized for the *"four D's"* – dull, dirty, dangerous, and distant chores. In the area of food processing and production, robot assignments are mostly picking and placing food products and packages [**126, 1**]. In these processes, the accuracy of the gripper's position and applied grasping force are important. Inappropriate gripper position or grasping force may cause the product's bruising and damage or loosening of the grasp. In the case of packages manipulation, this problem is relatively simple to resolve, as the package's shape and mechanical properties are usually known, constant, and can be designed to easily fit to a manipulator, or vice versa. On the other hand, picking and placing food products is a more complicated and sensitive procedure. The great variety in the product shapes, sizes, and structure poses a major problem in the development of manipulators [**93**]. Using an intrusive grasp, where pins are inserted to the grasped object, is generally not suitable for food handling, due to the possible damage to the product. Therefore, surface attraction grippers are much more common in food handling [**93**].

Automation is in vast use in agriculture, as well as in food production. Although in agriculture, processes like recognition, identification, approach, grasp, and manipulation of the objects are slightly more complex to perform. This is due to the inconsistency of the product's size, shape, hardness, position, orientation, and order along the "manufacturing line". As a result, the automated processes applied for low dexterity operations, usually manipulate the mass flow of materials, rather than selectively handling specific objects. This is obviously seen in the known field routines such as harvesting wheat, cotton, and corn [**14**]. Additional examples include the fruit-trees harvesters, which were developed in the form of: combines [**133**], auger shaped pickers [**72, 117**], tree shakers [**73**] and foliage shakers [**132, 134, 135, 39**].

Selective fruit picking is a very precise and complicated task that requires great dexterity; therefore it is performed by human fruit pickers. As robots and automated machinery replace human workers in many industrial fields, there have been attempts to automate this task as well. The fruit are varied and picked in different ways. For example, citrus, avocado, persimmon, cucumber, and sweet

peppers (70%) are harvested by cutting off their stem [**141, 20, 28, 51**], while on the other hand apples and mangoes are harvested by twisting and pulling them off the stem [**12**]. Consequently, an assortment of manipulators was developed, corresponding to the different harvesting methods. The basic manual tree growing fruit picking tools are equipped with a fixed curved blade whose aim is to cut off the fruit's stem, and drop the fruit into a small cage, as can be seen in the US patents [**9, 62, 65, 69**] and the commercial tool [**18**]. These configurations can be improved by adding a twisting blade to cut off the stem, or a sleeve that drains the fruit into a container, positioned on the ground [**141, 16, 70, 74**]. Utilizing robots as selective fruit pickers began in the 1950s, following the increased usage of electronic systems and computers. Most of the developed systems were manually controlled hydraulic manipulator arms, with two to three DoF – linear and rotational [**131, 17, 94**]. The arm's end-effectors varied from a simple static fork used to pull the fruit off the branch, through one DoF clamp gripper – with or without stem cutting blades [**141, 28, 76**].

The basic robotic grippers lack the desired grasp precision of the fingertip position and delicacy of the applied grasping force. These parameters are coupled due to the relation between the deformations and stresses, of both the grasped object and the gripper's fingertips. Therefore, developments in manipulators for compliant objects and especially in agriculture and food industry, include different types of force and position feedback, in order to achieve grasp control [**78, 50, 38**]. One solution is the use of grippers with deformable fingertips – like foam, rubber, or inflatable cushions. This solution provides a compliant contact surface that distributes the applied grasping force upon it. The bruising of the object due to concentrated contact force is reduced or prevented. Some of the gripper designs utilize this concept, and utilize inflatable rubber pockets [**55**], or magnetorheological fluid[1] pockets [**91**]. A different approach is to precisely control the gripper's finger position or the applied grasping force [**44, 107**]. This approach is more complicated to implement, as it requires a high degree of performance control utilizing precise feedback sensors and actuators. The feedback sensors can perform measurements on the actuated force, or the position of the object and fingers. Force sensors can be placed at the fingertips [**38, 78**] or at the fingers base or joints [**119**]. The object's position measurements can use image processing, by utilizing monoscopic or stereoscopic vision systems. Further, the cameras can be positioned on the manipulator base [**28**], on the end-effector [**76, 49**], or both. A laser scanner can also be used for distance measurement [**12, 94, 4**].

Traction is essential for grasping and object manipulations. It is commonly achieved in industrial grippers by using suction cups [**95, 93**], or clamps with a foam or rubber layer at its ends. Even though some different and interesting approaches and techniques for grasping are available: Festo FinGripper© [**36**] – is a gripper constructed of two or more single DoF fingers, each of which is a chain of four-bar mechanisms. The "freezing gripper" – which freezes vaporized water by a cooling nozzle and by that maintains an adhesive grasp [**66**], and a non-contact gripper utilizing the venturi air flow effect [**31**]. An innovative approach is a gripper made of a cushion filled with granular material. It provides a universal shape gripper due to the amorphic shape and flexibility of the cushion, while it presses onto the object. The granular material provides the firmness and the grasp force as it quickly contracts and solidify when vacuuming the cushion [**82**].

[1] A magnetorheological fluid is a material where the rheological properties change when a magnetic field is applied [**91**].

2.2. Grasp Models

The grasp model includes kinematic, dynamic, and contact models [**112**]. The kinematic model defines the system's mechanical constraints, the dynamic model defines the dynamic behavior of the system's elements [**118**], and the contact model defines the coupling between the object's and the gripper's force and torque reactions to their deformations [**137**].

An object's grasp can be achieved by constraining it using a number of contact points [**140**], a contact surface [**116**], or by geometrically *caging* it [**124, 21**]. Each of the described methods requires a different grasp model. This work concerns and deals with the first method.

In order to describe and characterize the grasp model, several parameters are defined: the grasp type, the contact model, the grasp stability, and its basin of attraction. The grasp type describes macro scale parameters, such as the *closure* of the grasp, the number of contact points, and the object's and gripper's geometries and dimensions. The contact model, on the other hand, deals with micro-scale properties of the grasp, which are the reactions, deformations, and motions between the two contacting bodies – here, the object and the gripper. The grasp's contact models are reviewed in the following subsection 2.2.1, while the grasp's type, stability, and basin of attraction, are reviewed in section 2.3.

2.2.1. Contact Models. The contact models aim is to assess the reactions at the contact point of two bodies, and their correlation to the bodies deformation. The variety of contact models differ by the considered assumptions on which they are based. Derived contact models consider no slip between the surfaces while in contact.

A rigid contact model, i.e., assuming the contacting bodies as rigid, raises obstacles to the grasp's analysis. First, the equations of motion are insufficient to provide all reactions, due to the system's static indeterminacy. Therefore, the grasp's analysis is defined solely by kinematic constraints, which are described in section 2.3. Further, this contact model leads to consideration and modeling of phenomena such as *Impact* and *Dynamic ambiguity*.

Impact is a phenomenon that occurs between colliding rigid objects, and causes energy loss [**10, 11**]. Collision of rigid objects is modeled as elastic collisions, which is described by the conservation of linear and angular momentum. In reality, the rigid model is insufficient to describe the interaction, mainly due to impact, plasticity, and friction. In order to "tune" the rigid body model, the momentum conservation equations are factorized by: e - *the coefficient of restitution*. As described in [**129**] and further detailed in [**10, 48, 68, 120**], three different *impact models* were previously used to assess e. *Newton's kinematic hypothesis*, or *Newton's law of impact*, defines the coefficient of restitution as the ratio of normal relative velocity at the contact point, before (c_i) and after (c_f) the impact, $e = -\frac{c_f}{c_i}$. This method was extended in [**11**] for a three-dimensional problem. *Poisson's hypothesis* [**102**, p. 150] states that the impulse in the restitution period is e times that in the compression period. Denoting the normal and tangential impulse force components P_n, P_t, yields that $e = (P_{n,T} - P_{n,c})/P_{n,c}$, where $P_n = P_{n,c}$ at the end of the compression phase and $P_n = P_{n,T}$ at the end of the impact. Based on the above, a systematic method for analyzing impact problems was developed by [**130, 129**]. The *Energy hypothesis* or the *internal dissipation energy hypothesis* as suggested in [**120**], defines the coefficient of restitution as $e = \sqrt{E_{rel}/E_{abs}}$, for the energy released at the contact during restitution E_{rel} and the

energy absorbed during compression E_{abs}. Although the resulting analytical expressions are somewhat complicated, the last approach is the most satisfying when regarding non-frictional energy loss.

Another phenomenon of the rigid body model is the *Dynamic Ambiguity*. For simplicity, consider a planar mechanical system of a rigid body with frictional contact [**85, 86, 25, 27**]. The dynamic solution of such a system depends on the *contact modes*, which are different reactions at the contacts, described by the constraints on the corresponding contact force and relative velocity. For two planner rigid objects, four contact modes are defined for a contact point: **S**eparation, **F**ixed to (or roll on), and relative slide to the **R**ight or to the **L**eft (S,F,R,L). The contact modes are instantaneous and add two time-dependent constraints equations and inequalities, to the equations of motion [**85**, p.75]. In that manner the equations of motion are integrated while applying the constraints that define the contact mode. The contact point behavior and the corresponding contact modes switch during the solution of the system. The appropriate contact mode is selected by continuously checking all four modes and selecting the feasible one. It happens that more than one contact mode is feasible for a certain system's configuration, so the system's dynamics is ambiguity and its behavior cannot be analytically defined. In [**85, 86, 87, 88**] the dynamic ambiguity is implemented into the walking plan algorithm for a multi-legged robot. For each set of contact points, the algorithm computes the possible locations of the robot's center of mass that may cause each contact mode. In that manner the robot can maintain its stability by not slipping, and select the robot's configurations to be where the dynamic ambiguity is avoided, and the system's behavior can be predetermined. The dynamic ambiguity is resolved when considering the compliant contact model, due to the deformations and forces coupling [**116, 129**].

Considering both bodies as quasi-rigid and compliant means that the deformations due to compliance are localized to the vicinity of the contact point [**64**]. The quasi-rigidity assumption is generally valid for bodies that do not contain slender substructures, and bodies that are not exceptionally soft [**139**]. The compliant contact model complicates the grasp analysis, due to the coupling between the applied grasping force and torque to the object's and the gripper's deformations. On the other hand it enables computation of the applied grasping force. The first contact model for compliant (*deformable*) objects was introduced by Heinrich Hertz in 1881 [**52**, p. 146][**53**]. The Hertzian model provides an analytical solution of the deformation and stress distributions of two identical, homogeneous, isotropic, elastic, and perfectly smooth spheres, under solely normal compression. It is worth noting the following: the normal direction is defined along the line connecting the two spheres' centers – before the deformations; the contact area is small relative to the body's dimensions; the common contact surface, which is an outcome of the body's deformations, is assumed to be a general ellipse shape. Extension to the Hertzian model was derived by Mindlin [**81**] in 1949. His extension considered two elastic elliptical bodies in a three-stage load. First, they compressed along the line that connects their two centers (the normal), next they are loaded with tangential force – perpendicular to the normal, and finely loaded with a torque about the normal. Mindlin shows that micro-slip occurs at part of the contact area. Further, he showed that the tangential compliance is between one to two times greater than the normal compliance – as long as there is no slip, and he presents the stress distribution due to the applied torque for a circular contact area.

A different approach was introduced by Walton in 1978 [**127**]. For the case of two identical elastic spheres under an oblique loading profile[2] while assuming no slip at the contact area, he derived the

[2]For the normal and tangential deformations δ_n, δ_t. The oblique compression is given as $\delta_t = c \cdot \delta_n$, where c is a constant.

relation between the contact area displacement and the stress distribution along it. Walton used the *energy flux criterion* in order to achieve a unique solution without singularities at the edges of the contact area. If to denote the line connecting the spheres' centers as the z-axis and the oblique compression along the $z-x$ plane, the energy flux criterion is the physical phenomenon – where there is zero net flow of energy between the spheres. It follows that any energy flux that does exist will be symmetric in the y direction and non-symmetric in the x direction. In comparison with Mindlin's work, Walton shows that if slip does exist it will be in the form of sliding of the entire contact area, and that the slip is strongly dependent on whether the spheres are first compressed and then sheared, or compression is performed in an oblique manner. Walton extended his work [**128**] to calculate the overall moduli of elasticity of random packing of spheres. He considered the initial deformed state of the spheres and two frictional cases: where the spheres are infinitely rough or perfectly smooth. Walton's papers [**127, 128**] were re-derived in a simple straightforward manner by Elata [**29, 128**]. Elata discussed the contact force-displacement relations, and shows that misuse of that relation leads to violation of the second law of thermodynamics. He points out that the dissipation of energy in the elastic deformation cycle is known and physically reasonable due to friction. But, the energy dissipation as it emerges from Walton's equations under the cyclic loading path, is caused due to misuse of these equations, and results in energy generation when performed in the opposite direction. That is physically impossible, as it suggests that energy is generated while no work was done – where the elastic potential cycle is assumed. Overcoming this models problem, Elate expanded Walton's model for an arbitrary loading trajectory by adding a configuration parameter that comprises the energy dissipation. Elata's model considers nonlinear elasticity and energy dissipation in the tangential direction, and does not consider the torque reaction.

An anthropomorphic soft finger contact model was studied by [**139, 56**]. They suggested that the radius of contact of a soft finger is proportional to the normal force raised to the power of α. α ranges from 0, corresponding to the "ideal soft finger", to 1/3 which corresponds to the linear elastic contact model derived by Hertz [**53**]. Experiments and a finite element method (FEM) analysis were conducted to verify the theoretical model [**138, 139, 57**], and further the forces reactions at the contact point due to the material's viscoelasticity [**122**]. This study showed that the typical human α values are 0.11 and 0.17 for the thumb and index fingers, respectively.

A simplified first order contact model, which models the contact reactions as a spring and damper system, is sometimes used in order to achieve analytical proof of the grasp stability. In this model, the spring represents the contacting bodies combined elasticity, while the damper represents the contact's energy dissipation. Based on this model, a framework for analyzing dynamic stability of a rigid object, grasped by compliant fingertips, was formulated by [**137**]. They showed, based on Lyapunov's direct method, that the whole dynamic system is asymptotically stable in the vicinity of the equilibrium position, if its impedance matrices are positive definite. Further, they presented a quantitative measure for comparing the dynamic stability, and showed how this stability is influenced by the contact forces of fingertips, the resultant curvature radius at each contact, and the area of the grasp triangle – formed by the three points of contact (for tree finger grasp).

A compliant contact model based on a variational method as in finite element analysis, is proposed in [**116**]. They discretized the contact area and analyzed the normal and tangential complaints and stresses, while considering the micro-mechanics of friction. In order to overcome the difficulty of the exceeded number of unknowns versus the number of prescribed constraints, an optimization based on

minimizing the system's potential energy was used. Due to the "either/or" conditions in some of the constraint equations, Schittkowskis algorithm was combined with the analytical model. Minimization of the potential energy of the finger/object system was chosen, since the interactions between the finger and the object are modeled as an elastic phenomenon, which follows that the stresses and deformations act in such a way that minimized the total potential energy of the system. This model allows relatively large deformations; the object can be arbitrarily shaped, there is no limit on the number of fingers that grasp the object, and the changes in forces do not need to follow a particular profile. The model in [**116**] was integrated with the Herzian model in [**136**] for the enveloping grasp and the prediction method of passive force closure. They used the Levenberg-Marquardt method to obtain the local elastic deformations, and a natural model of contact compliance to predict the corresponding passive contact forces. The work done in [**40**] utilized FEM to extended the form closure[3] framework to a class of deformable objects. They modeled a grasped object as a linearly elastic frictionless polygon, using a finite element mesh with a corresponding stiffness matrix. They defined the free space as the subspace of the mesh's node configuration space, which keeps the mesh topology and does not include the collisions with the rigid fingers. Next they defined that the grasped object is in *deform closure* if positive work is needed to be applied on the object, in order to release it from its grasp. Based on the node's displacement and the stiffness matrix, a potential energy function was suggested as a measure of the deform closure quality.

2.2.2. Organic Matter Models and Analysis. It is important for robotic harvesting to determine the safe handling limits for the specific crop during harvest and in post-harvest processes [**19**]. Defining these limits for organic matter complicates the analysis due to the indeterminate values of the object's mechanical properties, such as its geometric shape, mass, Youngs module, shear module, Poisson's ratio, and yield stress. Further, as the organic matter is not homogeneous and is anisotropic [**60**], the values of these parameters change from one point to another in the object's volume, and along time. In order to assess these parameters and to model their change due to environmental factors, a series of experiments and measurements have been conducted. Oranges are surveyed by measuring the force needed to compromise the peel, either through puncture or bursting [**5**]. Experiments use several diameter punches or a plate, and the system is mounted in a press testing machine [**104, 19**]. The experiments outcomes are force-movement plots, which enable assessment of the object's general Young module and yield point. These parameters are measured using similar methods for smaller fruits, such as Blueberries [**103**]. Flowers stems' mechanical properties are assessed by testing their strength in bending – by using three-point loading, and their strength in compression – by using two plates pressing in the direction of the stem's radius [**115**].

A non-destructive approach to assess fruit firmness is by testing the fruit's vibration attenuation characteristics. In this method the fruit is vibrated using a random noise generator, and vibrations within the fruit are measured by filtering the signal from an accelerometer or by Piezoelectric film. The ability of fruit to transmit frequencies greater than a certain frequency decreased as the fruit softened [**32, 58, 83**]. This method yields a *Firmness Index*. It is not as reliable as the pressure test, but it can be correlated to the Young module, as described for apples, pears, and peaches in [**37**], and it has an advantage as it is nondestructive [**33**].

Further detailing the stresses and deformation in organic matter, is done by performing a Finite Element Method (*FEM*) analysis. This method was used by [**77, 47**] to predict the internal stresses

[3]Detailed in section 2.3.

and deformations of melons. In [77] the melons were subjected to handling by two types of grippers: parallel plate and v-v notch grippers. Numerical values of Young's module of elasticity used at the FEM was measured for the inner, middle, and outer portions of the melon by using flat plate compression of cylindrical samples. The melon rind's module of elasticity was determined by performing a tensile loading test. They showed good correlation between the FEM analysis to the experiments, and further it gave better predictions than the Hertz's contact model. In [47] the FEM was assessed by performing a resonance sonic test – as described above. They investigated the influence of the melon's water core to its resonant frequencies, and constructed a four-layer FEM mesh model. The FEM analysis was used to model the firmness of carrot and cucumber [61], apples, and pineapple [45, 46]. All of them used the resonant frequencies test to validate the model and to assess the fruit/vegetable firmness by defining the Firmness index and Youngs module.

Other studies were performed to define and assess the critical damages, and their influence on the organic object's mechanical properties and organic condition [125]. In these experiments they measure the respiration, weight loss, percent decay, and a dye score, related to abrasive damage of the organic object. The damages were surveyed along the production line – from harvesting to distribution, and consider mechanical damages such as bruising, and environmental conditions such as temperature and relative humidity.

2.3. Grasp Stability Analysis

A grasp is said to be *stable* if it is in an *equilibrium grasp*, meaning that the grasped object remains statically grasped while an external force and torque can be applied to it. It follows that a *grasp basin of attraction* is the set of all the forces and torques that can be applied to the object, from which the grasp will converge to an equilibrium grasp [109, 99, 98].

While considering the grasp of a rigid object by a rigid gripper, different types of grasp closures can be defined in order to describe the gripper and object system. The grasp closures can be divided into passive and active closures, which are concepts that aim to describe the constraining mechanisms. An *active closure* is where the gripper can apply any force and torque to the object in order to maintain the grasp. A grasp is said to be a *passive closure* if the grasped object position and orientation remain the same, even when an arbitrary external force and torque are applied on it, while the constraining mechanism's joints-drivers remain constant as well. The passive closure is further divided into *passive force closure* and *passive form closure*. The former is where a preliminary constant contact force is needed to achieve grasp, and the latter is where this force is not needed – solely kinematic considerations [6]. A unified theoretical framework for robotic grasping and manipulations is provided by [140]. He defined and classified the active and passive, form and force closures for rigid objects and grippers. Further, while considering both frictional and frictionless contact points, the necessary and sufficient conditions for the minimal number of contact points needed in order to hold each closure, were introduced for a spatial three-dimensional space. The consideration of friction implies that the grasping force can be applied in the tangential as well as in the normal directions, relative to the plane tangent to the object's surface at the contact point. An extension for n dimensional space is introduced as well. The passive form closure is further analyzed in [6], for the concept of an adaptable fixturing system. Analyzing the grasp while considering the object's perimetric curvature and not only the tangent plan at the contact points, was introduced by [96, 97, 99, 98]. They analyzed the influence of the considered perimetric order to the passive form closure, and to the number of fingers

needed to achieve it. They further defined the first and second order mobility index to estimate the equilibrium grasp quality. The passive force closure is studied in [**114**] for the set of external forces and torques that can be applied to the grasped object while maintaining an equilibrium grasp.

Analyzing grasp stability of a non-rigid object and gripper is greatly affected by the contact model. It is worth noting that while considering a non-rigid contact model, the grasp is by definition an active force closure. Following [**127**] and [**140**], the conditions for the existence of *passive force closure* in a rigid object grasped by a compliant gripper is characterized in [**111**]. They further introduced *passive stability* as the set of external wrenches that can be passively resisted by the grasp. It is shown in [**136**] that the compliant grasping system is stable when the compliant matrix is positive definite. This matrix comprises the local geometrical properties such as relative curvature tensors, the material properties at contacts, and the grasp configuration. Further, in [**112**] an analysis of a frictional nonlinear grasping model is described, and it is shown that such grasps are not governed by any potential energy due to the asymmetrical form of the composite stiffness matrix.

A phenomenon that must be considered in the grasp stability Analysis is the *stick slip*. It occurs between two contacting bodies that are under normal and tangential loads. When the friction force between these bodies reaches a threshold, it can no longer sustain the static equilibrium with the external tangential load, and the bodies begin to slip over one another. When the tangential load is very close to that threshold, the system switches in a rapid cyclic manner between the two states [**23**]. In order to prevent or to reconcile this unstable phenomenon with the control law [**121**], it is important to know the critical friction force. The Coulomb's friction model is commonly used to describe the static friction force. It defines this threshold as proportional to the applied normal load – while the proportion is defined by experiments, per material combinations [**25, 27**]. Spatial geometric representation of this threshold is referred to as the *Friction Cone*, where the cone height is the normal load, and its basis radius is the threshold amplitude – at the contact point [**109, 112, 140**]. It is said that as long as the applied force is inside the friction cone, the two contacting bodies maintain stuck together – or perfectly adhesive. The cones at the contact points and their intersection are used in the grasp stability analysis to describe the equivalent geometric space to the allowed external loads that will not result in crossing the threshold and keep the desired grasp closure [**85**]. A poly-sided pyramid can be used as a simplified linearization of a cone, where its polygon base is inscribed in the circular cone base [**2, 79**]. Due to its definition and discontinuity, the Coulomb friction law may not lead to a unique static or dynamic solution, as described in [**87, 88, 116**] and in subsection 2.2.1. A different approach to avoid the stick-slip phenomenon is by applying feedback PD or force control, based on the bodies relative velocity [**24, 26**].

Coin snapping is a phenomenon that occurs when applying excess grasping force to an object. That force may cause the grasp to lose its stability. When considering a rigid body contact model, the system's stability can be verified by using Lyapunov's function [**118**]. Further, assuming that the object's external loads are derived from a potential function, the Lyapunov function candidate can be constructed of a linear combination of that function and the object's kinetic energy. Now, in order to show that the system's equilibrium point is stable, it is possible to show that the energy function has a minima at this point in the configuration space. This is achieved by ensuring that the first derivative of the Lyapunov function by the configuration parameters is equal to a vector of zeros – at that point. Further, in order to verify that this is a minima extremum, the second derivative of Lyapunov function at its parameters has to be a positive definite matrix. After performing the second

derivative, it is possible to see that the matrix becomes singular and even negative definite when the external loads exceed a certain threshold. This implies that the equilibrium point is no longer stable, and any minor disturbance will cause the object to loose its grasp.

The human hand is widely studied for its grasping diversity, which is due to the palm's dexterity in its twenty-seventh DoF. Thirty-three different grasp types are generally defined, which can be hierarchically arranged into seventeen grasp types [**34, 35**]. This research proposal is concerned with the general definitions of grasping. As the human grasp is of course compliant, it automatically defines it as an active force closure; the human grasp is briefly mentioned here due to its special and varied capabilities.

2.4. Grasp Synthesis and Planning

Based on the chosen contact model and the system's mechanical properties, it is desirable to define the appropriate grasp type and formation. This includes deriving the number of grasping points, and their position and/or applied force, so that the object will be firmly grasped and undamaged by the gripper. This problem is difficult to solve since there is a large number of possible solutions, due to the large number of variables and their complex relations.

The space of possible stable grasps is too large to search exhaustively [**42**]. In order to drastically reduce the search space, the 3D object can be approximated by decomposing it into shape primitives such as spheres, cylinders, cones, and boxes. A set of rules can be used to generate a set of grasp starting positions and pregrasp shapes [**80**]. This concept was improved in [**42**] for a multi-level superquadric decomposition method. In this method, the 3D object is decomposed into simplified superquadric primitives organized in a binary search tree. The tree's nodes are the simplified superquadric primitives, and the tree's level defines the decomposition's detail level. For grasp planning, superquadrics have the advantage of encapsulating not only the approximate volume of the original object but also approximating surface normals; further, they are convenient to work with as they are convex and symmetric. The found grasp solution is determined for a predefined gripper and it is not optimal due to the finite tree's level, and as the search effort is bounded to a total-fit error threshold. Following the decomposition, the grasp planning solution is found using Support Vector Machines (SVM) [**90**]. This method provides a measure of approximation to the grasp quality, which enables a selection of an optimal grasp from the space of the object's grasping parameters. The algorithm is used to build a regression mapping between object's shape, grasp parameters, and grasp quality. Once trained, this regression mapping can be used very efficiently to estimate the grasping parameters that obtain a highest grasp quality for a new query set of superquadric shape parameters. These methods were integrated into the grasp planner of the eu GraspIt! project [**79, 3**], in order to sample candidates for grasping simulations.

A search-table is a known method used to shorten calculation time, when fast or on-line calculation is required, while the numerical evaluations are too complex for the computing system. This method is used as a solution for grasp synthesis based on shape matching experiments. The issue of 3D model identification is treated in the field of computer graphics as well as in grasping, and so it follows that some of these works are related and complementary. Some known 3D model databases were published by: Osada [**89**], MPEG-7 [**142**], Hilaga [**54**], Technion [**71**], Zaharia [**143**], The Princeton

Shape Benchmark [113][4] and the Colombia Grasp Database (*CGDB*) [43]. CGDB includes several hands, thousands of objects, and hundreds of thousands of grasps. Further, [43, 41] describes the database and a grasp planning algorithm that exploits geometric similarity between a 3D model and the CGDB objects. Their similarity is defined based on L^2 distances between the Zernike descriptors of the object and the database. Zernike descriptors are invariant parameters, which are the projection of the function defining the object onto a set of orthonormal functions within the unit ball, introduced as the 3D Zernike polynomials by [13]. These descriptors hold properties such as invariance under scaling, rotation, and translation. They possess descriptive power, providing a basis for similarity measures between 3D objects, which is close to the human notion of resemblance [84]. The outcome of their algorithm is an appropriate form of closure grasp planning.

Machine learning for guided grasping enables learning how to grasp unfamiliar objects by evaluating sensory information and image processing. Based on statistical analysis for off-line selection of heuristic strategies and quality predicting, [67] and [92] present a general scheme for learning sensorimotor tasks, which allows rapid on-line learning. This is followed by generalization of the learned knowledge to unfamiliar objects. The learning is based on a routine of generating grasp candidate actions, and then estimating their quality, until a satisfactory performance grasp is found. In [101], the developed technique was based on separately learning the local (geometrical) and global (physical) properties by the grasping criteria of each object. In addition, high level criteria for human grasps are, for example, the material of the object's surface and the role of the grip, i.e., the role it plays in order to do further operations, e.g., grasping a cup at its bail in order to drink something, or a sledge at its handle to bang a nail into the wall [101]. These high level criteria are usually not considered in grasp planning. A *simulated re-annealing* method was suggested by [15] based on the work done by [59]. This method statistically finds the best global fit of a nonlinear non-convex cost-function over a high dimensional space. Its stochastic nature spares computation of the energy gradient, and provides the possibility of an uphill move to a state of higher energy, which allows it to escape local minima – unlike greedier methods. Further, the algorithm works well on non-linear functions. Due to the random exploration of the high dimensionality input, the computational efficiency of this algorithm is diminished. In order to increase the computational efficiency, it is suggested in [15] to perform the search in the *eigengrasp space* and not in the DoF/configuration space. It is shown in [108] that most human grasping postures are derived from a relatively small set of discrete pre-grasped shapes. Therefore, a much lower dimensionality parametric space – the eigengrasp space, provides a very good approximation of the grasp, compared to its description in the configuration space.

2.5. Computer Simulations and Experiments

Computer simulations enable the calculation and prediction of parameter values based on a derived theory. One of largest test beds for grasping simulations is "GraspIt!", developed in the Computer Science Department of Colombia University [79, 3]. GrspIt! is an interactive grasping simulator that can import a wide variety of hand and object models, and can evaluate the grasps formed by these hands. It features: *a*) a robot library that includes several hand models, a Puma arm, and a simplified mobile base; *b*) a flexible robot definition that makes it possible to import new robot designs; *c*) an interactive interface, as well as an external interface to MATLAB; *d*) a fast collision detection and contact determination system; *e*) grasp analysis routines that evaluate the quality

[4]Some more 3D model databases are reviewed in [113].

of a grasp; *f*) a dynamics engine that computes robot and object motions under the influence of external forces and contacts; *g*) a simple trajectory generator and control algorithms that compute the joint forces necessary to follow the trajectory. Some of the research that utilized GraspIt! for grasp analysis, synthesis, planning, and their presentations are [**43, 42, 41, 80, 90**]. Another platform is the Princeton Shape Benchmark(PSB). It is a database of polygonal models that were collected from the World Wide Web and a suite of tools for comparing shape matching and classification algorithms. It features multiple semantic labels for each 3D model. For instance, it classified the 3D models based on their function and form, or based on how the object was constructed, e.g., man-made versus natural objects [**113**].

As well as a whole grasp assessment, FEM simulations are performed in order to assess micro-scale parameters such as the contact models. FEM is a numerical procedure, especially suited for solving the partial differential equations that describe stresses, strains, and deformations in materials. Since it is a numerical method, it can be utilized for both static and dynamic analyses, and allows modeling of irregularly shaped objects, which obtain nonhomogeneous properties, and are subject to mixed boundary conditions. The models are validated by comparing their results to performed experiments. When a good model to experiment correlation is achieved, the model is used to analyze and predict the results of more complicated configurations [**116, 136, 40, 77, 47, 61, 45, 46**].

Experiments are performed in order to obtain material properties, and to validate the simulated model. Desired material properties are usually its Young module, Poisson ratio, and the yield stress. Performed experiments for obtaining organic matter's properties are detailed in subsection 2.2.2. In order to validate a compliant contact model, the constructed experimental system included a soft hemispherical object, a micrometer for position measurements, and a load transducer. In these experiments, the relation between the applied load – normal and tangential, the movement, i.e., the objects deformation, and the resultant contact area are measured. The contact area was measured using two methods: the first is by stamping the object onto a micrometer paper – and measuring the remaining ink marks [**139, 138, 110**], Figure 2.1(a). The second is by pressing the object onto a transparent glass, and using the contact area's reflection directly [**63**] or by image processing to detect the contact areas edges [**123**], Figure 2.1(b).

The relaxation response of viscoelastic materials when the grasping is under position control, is a contact interface that has been widely used in soft robotic fingers, robotic feet, and robotic arms. It was studied by applying force control to a silicone model, and measuring the creep phenomenon using a high-speed camera as a vision sensor [**122**], Figure 2.1(c).

Grasp stability and closure have been experimentally tested as well. In [**109**], a two-dimensional object grasped in a passive force closure was tested for its stability margins under external load. The two linear-linear DoF grasping compliant fingers, were passively centered by springs, and mounted with a load transducer at its end, so the applied grasping force can be measured, Figure 2.1(d). They further measured the coin-snapping phenomenon – which is the loss of stability due to excess grasping force. The coin-snapping phenomenon is further detailed in section 2.3.

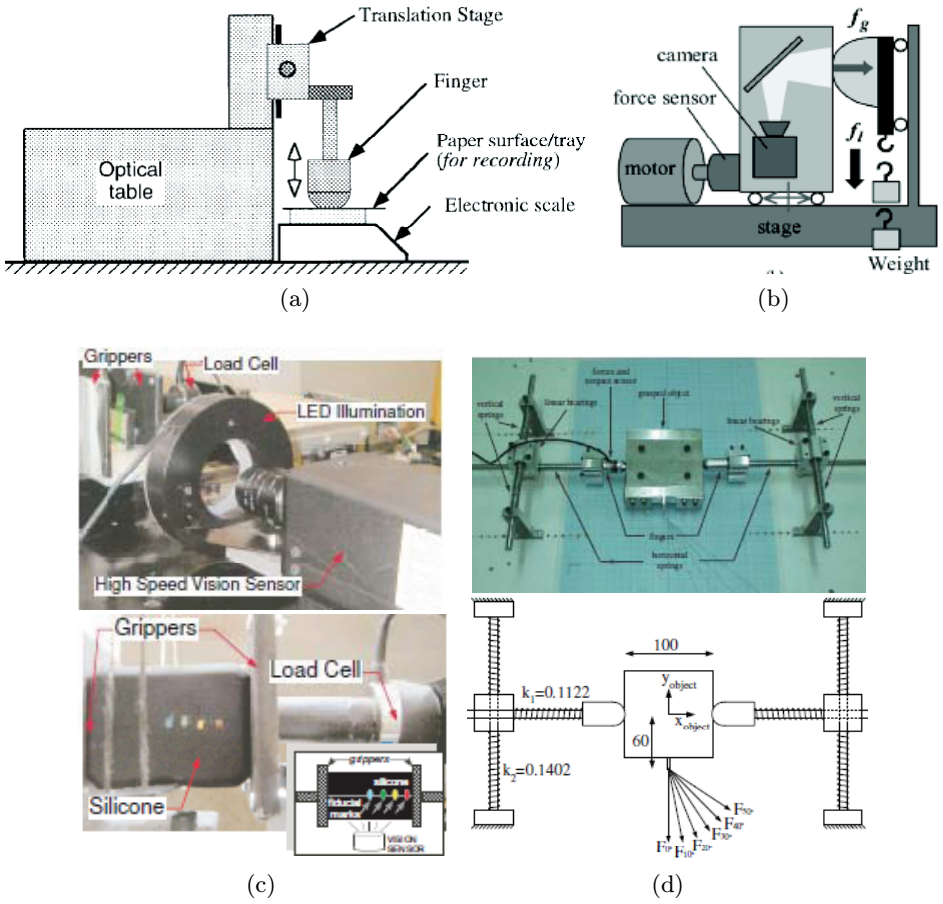

Figure 2.1: Experimental systems by: (a) Xydas [**139**]; (b) Ueda [**123**]; (c) Tsai [**122**]; (d) Shapiro [**109**].

CHAPTER 3

Methodology

3.1. Overview

In this thesis, an optimal grasp of compliant objects synthesis will be developed, Figure 3.1. The basic step, as detailed in section 3.2, is to construct a full dynamical system, including the gripper's and the object's dynamics. Assuming the gripper's fingertips and the object as compliant (or quasi-rigid), a soft finger contact model will be used, based on Elata [**30**] or Kao et al. [**139, 138, 122**].[1] The contact model will describe the contact points force and torque reactions, and their relation to the local deformations. The following parameters are defined and assumed as known: a set of objects $\tilde{B} = \{\tilde{b}_b\,;\, b = 1 \dots nb\}$ defined by their geometries and their mechanical properties. For each object $\tilde{b}_b$ there are a set of external forces and torques (*loads*) that can be applied to it $\tilde{F} = \{\tilde{f}_j\,;\, j = 1 \dots nj\}$, and a set of grasp configurations $\tilde{K} = \{\tilde{k}_k\,;\, k = 1 \dots nk\}$. Each $\tilde{k}_k$ configuration is defined by a set of $\{i\,;\, i = 1 \dots ni\}$ contact points. A *system configuration* is defined to be a specific object $\tilde{b}_b$, grasped by i contact points in a configuration $\tilde{k}_k$, and loaded with an external force and torque $\tilde{f}_j$. The solution algorithm that will be developed in this thesis is described in Figure 3.1, and as follows: Given an object $\tilde{b}_b$ loaded with an external load $\tilde{f}_j$, grasped by i contact points in a configuration $\tilde{k}_k$:

1. Calculate a grasp quality value for the current system configuration, by solving the statically indeterminate equations of motion, while considering the physical constraints, section 3.3.
2. Calculate a grasp quality value for the current grasp configuration, by repeating step 1 for all $\tilde{F}$, section 3.3.
3. Search $\tilde{b}_b$'s circumference for an optimal grasp quality value, by repeating step 2 for varied $\tilde{k}_k$. This step yields an optimal grasp configuration in the sense of the defined quality criterion, section 3.4.
4. Repeat steps 1–3 for all $\tilde{B}$.

The grasp model will be assessed using computer simulation, and the results will be compared with an experimental system, section 3.5. The algorithm's outcome, i.e., the optimal contact points configuration and the corresponding reactions, could later be used as gripper design objectives.

3.2. Spatial Compliant Grasp Model.

All system parts will be assumed to be quasi-rigid. The kinematic model, and its subsequent dynamic models, will be constructed by using the transformations of rigid bodies method. Each fingertip, contact point, and center of mass position will be described by its fixed coordinate frame [**118**, pp. 29,187]. The grasp loading path of each contact point is the offset of the finger's frame off the nominal contact point. The corresponding local deformations are described relative to the local contact

[1] The models are currently studied for their properties and differences.

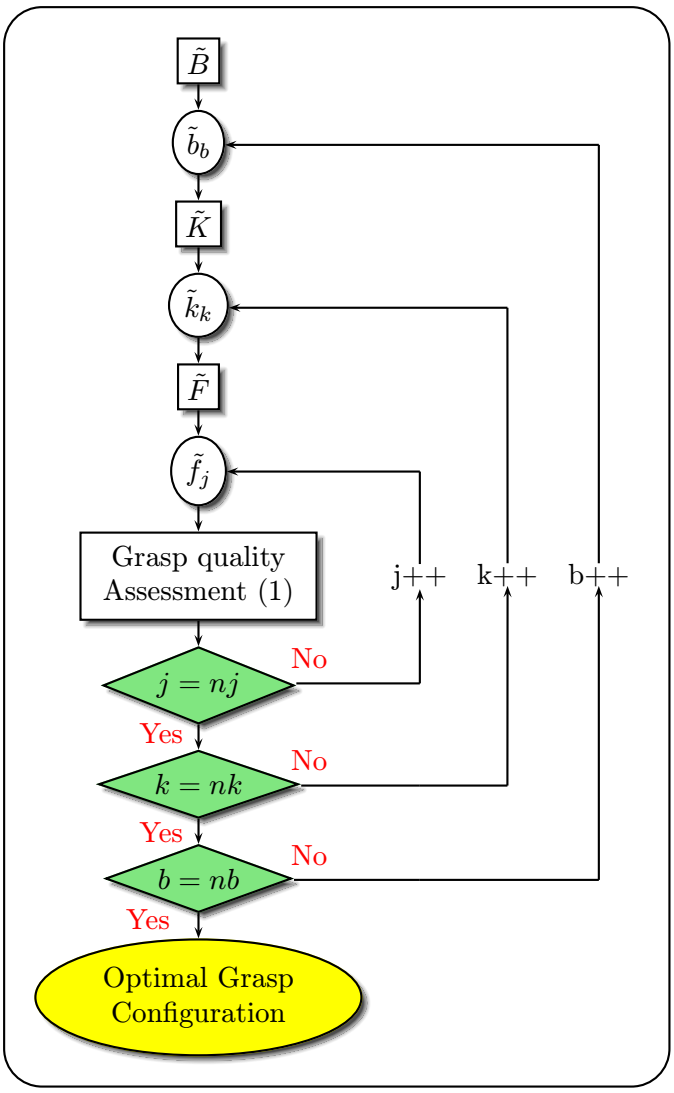

Figure 3.1: Optimal - grasp search algorithm.

point and fingertip frame. This method enables an easy transformation of values, to be represented in any reference frame.

At first, in order to maintain simplicity, the grasped objects will be modeled as convex closed shapes with a known surface function – superquadric for example. Further, the use of more complex shapes and their composition will be implemented, as in[**42**].

Two compliant contact models are currently considered for use in the grasping model. Both models are studied at this stage for their characteristics and accuracy.

1. The model derived by Walton [**127**] for the oblique compression of two elastic spheres. This model was expanded by Elata [**29, 30**] for an arbitrary loading trajectory by adding a configuration parameter that comprises the energy dissipation, as detailed in subsection 2.2.1. This model considers nonlinear elasticity, the energy dissipation in the tangential direction, and does not consider the torque reaction. The torque reaction will be modeled based on a spring and damper model, or the model described in Mindlin [**81**].

2. The model derived by Xydas and Kao [**139**, **138**, **122**] for anthropomorphic soft fingers. It is based on the Hertzian contact model, and expands it to include tangential and torque loads, based on nonlinear elasticity. In this model the *limit surface* is defined in order to assess the stability of contact, based on the torque and the tangential force. It further deals with large deformations.

Note: Although the contact models considered in this work are spatial, the contact load's trajectory in both models is planar. This means that the models do not deal with a spatial load trajectory curve.

3.3. Grasp Quality Criteria

The grasp quality criterion defines the extra necessary constraints that enable a specific solution to the statically indeterminate grasp system. The criterion further defines the configuration's grasp quality value. It is assumed that the following parameters are given and known: the object's $\tilde{b}_b$ circumference geometry, the set $\tilde{k}_k$ of positions of the ni contact points – on the object's circumference, the external load $\tilde{f}_j$ that is applied to the object, the object's and fingertips mechanical properties and their bounds of allowed local deformations. The allowed local deformation bounds and the contact model define the maximal force and torque reactions at each contact point. The contact points force and torque reactions that will provide equilibrium grasp will be calculated. In order to solve the system's dynamic equations, and obtain a quality criterion value for a grasp configuration – the algorithm's first step, a Min/Max problem is formulated and solved. The cost function, defined by the desired grasp quality criterion and the constraining equations, stems from the physical properties of the problem:

Physical Constraints

- The force and torque equations of motion must be satisfied, for equilibrium.
- The normal part of the force reaction is greater than or equal to zero, i.e., implies that there is a contact.
- The tangential part of the force reaction is smaller than its normal part times the coefficient of friction, i.e., the static Coulomb friction has not reached its critical value.
- The deformations/stresses due to the force and torque reactions must not exceed the defined bounds.

Grasp Quality Criterion - Target Function

1. A norm function of the minimal required force and torque reactions. Considered functions are the absolute maximal reaction out of the i^{th} contact points, or their sum of squares – refined with gains.
2. The maximal force and torque that can be applied to the object at the contact points, without losing its grasp's stability.
3. Characteristics of the frame – invariant features of a grasp's stiffness matrix [**75**].

3.3.1. Invariability of the Grasps' Quality Criterion. The aim of the grasp quality criterion, as described above, is to grade each grasp configuration so that an optimal grasp can be obtained. An optimal grasp is defined as a grasp that will provide the maximal grasp stability and robustness margins, while applying the minimal grasp effort. The grasp effort is calculated as the sum of the wrenches norms applied at the contact points. Two considered norm functions are L_2 and L_∞.

If to describe the b dimensional wrenches $\omega \in \mathbb{R}^b$ applied to an object at k contact points, the grasp quality criterion is calculated using each of the the two norm functions:

$$L_2 \text{ Grasp quality criterion} = \sum_{i=1}^{k} \left(\sqrt{\sum_{j=1}^{b} \left(w_j^2 \right)} \right) \tag{3.1}$$

$$L_\infty \text{ Grasp quality criterion} = \arg\max_{k} \left(|f_{n,j}| \right) \tag{3.2}$$

where $f_{n,j}$ is the force's element applied at the j contact point, directed in the normal to the local tangent plan.

It is important noting that the grasp quality criterion in (3.1) is invariant of a chosen coordinate system, as all wrenches are calculated with respect to the grasped object's center of mass. Differently the criterion described in (3.2) is coordinate system dependent. Although, the use of the L_∞ norm is justified twice. At first, the grasp analysis is done based on the contact points' local deformation – based on the contact point's coordinate system. As the object's damage due to grasp and manipulation is at our interest, it is logical to consider the applied effort in that directions as a grasp quality criterion. Second, this criterion is an upper bound to the local grasp effort, so by choosing a minimal normal force the grasp effort is minimized. It is easily seen when analysing the assumed Coulomb friction model

$$f_n \geq \mu \left| f_t \right| \geq 0; \quad f_n \geq \nu \left| T_n \right| \geq 0; \quad | \quad \{\mu, \nu\} < 1, \tag{3.3}$$

where f_n, f_t, T_n are respectively the normal force, tangential force and the torque applied at a contact point.

The third grasp quality criterion that is frame invariant, is described in [**75**]. They define a set of frame – invariant characteristic stiffness parameters, and provide physical and geometric interpretation for these parameters. They define a frame – invariant quality measure, that compare the principal translational and principal rotational stiffness parameters. Based on that approach, different grasp configurations are compared based on the worst – case stiffness of the grasps.

Based on these criteria, it will be possible to search the object's circumference for the optimal grasp configuration. Both grasp quality criteria are considered at this stage of the work, and their implications, possibly lower and upper bounds for a specific grasp configuration, will be further considered at a later stage.

3.4. Finding an Optimal Grasp Configuration

The next step, after obtaining the quality criterion for the current grasp configuration, is to find the grasp configuration where the grasp is optimal. For the two optimization criteria described in section 3.3, it means finding the configuration where the first grasp quality criterion is minimal, or where the second one is maximal.

This step – the search, is the research's main innovation and contribution. Instead of selecting a specific gripper, and searching for its optimal grasp configuration, the derived algorithm will provide the optimal grasp contact points, based on the grasp quality criterion and the object's

geometry and mechanical properties. The search – based on the first quality criterion, is defined,

$$\mathbf{OPTG_b} = \min_{\mathbf{k}} \left(\min_{\mathbf{j}} \left(\underbrace{\max_{i} \left(\min_{\tilde{f}_{i,\hat{n}}} \left(J\left(\tilde{F}_j\right)\right)\right)}_{\mathbf{a^*}} \right)\right). \tag{3.4}$$

where $OPTG_b$ is the b's object optimal grasp configuration. From the inside out: $\min_{\tilde{f}_{i,\hat{n}}} \left(J\left(\tilde{F}_j\right)\right)$ is the dynamic solution for the current configuration - the first algorithm step, so that a^* is the grasp's quality criterion of it. $\min_j(\cdot)$ is the criterion assessment of this configuration for all plausible external loads, and $\min_k(\cdot)$ is the search on the object's circumference for the optimal configuration.

At this stage of the work, the criterion-based optimization is performed only numerically. Therefore, the described methods will provide suboptimal solutions, depending on the discretization's resolution:

1. **Finite differences**. In this approach, each configuration will be variate in its close neighborhood, where each point of it will be assessed by the grasp quality criterion. A numerical gradient descent method will be used to "drift" towards the optimal solution. The finite differences approach is currently the preferred method.
2. **Stochastic approach**. In this approach, new states are generated in the random neighborhoods of the current state, with a defined variance, and the grasp quality criterion is assessed for each configuration [59]. It enables a nonlinear non-convex grasp quality criterion equation, and releases the need for gradient computation, which may cause convergence to a local minima.

An analytical approach that relates the grasp quality criterion to the system's parameters is considered. This approach should present a more direct search algorithm and shorten the search's calculation time. Currently, based on the assumption that all of the system's parameters are known, the analytical approach is considered to include logical considerations, which will be followed by an analytic gradient descent. Further, when considering a complex and non-convex object's geometries, a logic selection algorithm will be used in order to identify grasp configurations, that are potentially preferred for search initialization.

3.4.1. Analysis of Grasp Optimization. At this stage of the work, grasp optimization is planed to be a search for the positions of the fingers on the object's perimeter. Consider an object, whose perimeter/surface is discretised by n nods mash, and is grasped by k fingers. The basic exhaustive search, (also named brute – force\naive\uniformed search) yields with algorithm complexity of $\frac{n!}{k!(n-k)!}$. In this work, the search space is finite. Therefore, although this value is the upper bound for any algorithm complexity, its implementation is considered at this work, as it is under a feasible processing time. Reconstructing the search space into a *search – tree* or a *graph*, which follow by the use of more efficient algorithm, may not reduce the search complexity i.e., search time. The reason is that constructing the search tree is by itself an exhaustive search. Complexity reduction could be achieved by an educated guess of the search's initial conditions, based on the object topology e.g., concave edges, distance from the object center of compliance [75], and the relative position of the fingertips off one another.

Heuristic and metaheuristics[2] search algorithms such as *linear relaxation, simulated annealing* [41], and *genetic programming*, will not be considered at this work due to their inability to guarantee an optimal solution.

3.5. Simulations & Experiments

The optimal grasp configuration will be simulated in order to present its stability margins, robustness, and the contact point's reactions. The simulation code will be written in Wolfram Mathematica, and will include the kinematic, dynamic, and contact models. Grasp control is not in this works objectives; therefore a simple PD grasp controller will be used to control the virtual gripper, which includes a force and position control. Details on the code and the modeling are presented in section 3.6. Further use of the GraspIt! software [79] as a simulation tool is currently being studied for its properties and features. GraspIt! is an environment for grasp analysis and planning, and it can serve as a test bed for new grasp evaluation, grasp synthesis, and manipulation of planning algorithms.

3.5.1. Experiments' Objectives. A numerous experiments will be performed on two designed experimental systems, in order to achieve the following objectives:

1. Measure materials' properties under pressure: sheer modulus G, Poisson ratio ν, and the related young modulus E.
2. Measure coefficient of friction.
3. Verify the used contact model.
4. Verify the grasp's robustness analysis.

3.5.2. Experiments' Methodology. In order to achieve the described objectives, two experimental system are currently in design.

- **Experimental System 1: Measuring material properties and contact model verification, objectives 1–3.**
  In order to achieve the first objective, the measurement system will measure the force – displacement relation of two objects. The measured compliant object will be forced against two bases, a solid plate and a compliant hemisphere. It will be further forced in two directions, along the normal – defined by the plate or the tangential plane at the hemispheres' contact point, and along a perpendicular direction. The object will be mounted on a 6D force/torque gage, in order to measure all the reactions that are applied to it. The displacement will be measured by a LVD measurement unit. In order to applied the perpendicular displacement, the based plat could be moved on its plan using two motion screw. By performing standard force – displacement experiments, by using standard model, the material Young modulus E can be estimated. By applying normal and tangential loads, while measuring the tangential displacement, the materials' sheer modulus G can be estimated. Assuming the material as

[2] a search performed by iteratively checking for a new candidate solution, mainly utilizing stochastic methods.

Orthotropic, These properties are related to the Poisson ration through Hooke's law as

$$\begin{bmatrix} \epsilon_{xx} \\ \epsilon_{yy} \\ \epsilon_{zz} \\ 2\epsilon_{yz} \\ 2\epsilon_{zx} \\ 2\epsilon_{xy} \end{bmatrix} = \begin{bmatrix} \frac{1}{E_x} & -\frac{\nu_{yx}}{E_y} & -\frac{\nu_{zx}}{E_z} & 0 & 0 & 0 \\ -\frac{\nu_{xy}}{E_x} & \frac{1}{E_y} & -\frac{\nu_{zy}}{E_z} & 0 & 0 & 0 \\ -\frac{\nu_{xz}}{E_x} & -\frac{\nu_{yz}}{E_y} & \frac{1}{E_z} & 0 & 0 & 0 \\ 0 & 0 & 0 & \frac{1}{G_{yz}} & 0 & 0 \\ 0 & 0 & 0 & 0 & \frac{1}{G_{zx}} & 0 \\ 0 & 0 & 0 & 0 & 0 & \frac{1}{G_{xy}} \end{bmatrix} \begin{bmatrix} \sigma_{xx} \\ \sigma_{yy} \\ \sigma_{zz} \\ \sigma_{yz} \\ \sigma_{zx} \\ \sigma_{xy} \end{bmatrix}, \tag{3.5}$$

where $\epsilon_{ij}, \sigma_{ij}$ are the strain and stress at the j direction on the plane defined by the norman i. The ν_{ij}, G_{ij} are the Poisson ration and the sheer modulus at the corresponding directions. Note that the used contact model does not depends on Young modulus E, although it includes the sheer modulus G and the Poisson ratio ν.

The second objective is achieved by applying normal displacement at the normal direction, and then at the perpendicular direction until slip is achieved. Slip is detected when the perpendicular force measurement is decreasing.

The third objective is achieved by performing a load path. Meaning that a normal and tangential displacements will be applied in certain order, and the normal and tangential forces will be measured. The results will be compared with the theoretical model in [**30**].

- **Experimental System 2: Grasp Robustness Measure System, objective 4.**
  The experimental **system's gripper** design is based on the Barrett hand [**8**], Figure 3.3. It will be assembled with three fingers, each with three DoF. The fingers' links and DoF will be constructed of *Dynamixel AX-12* digital servo motor [**100**]. These motors are embedded with an internal microcontroller, enable position and torque control, and I/O communication of all the motor's parameters. Each fingertip will be mounted with a *Nano25-E* – a six-axis transducer, in order to measure the forces and torques that are applied at the contact points [**7**]. The transducer itself is mounted with a half sphere compliant fingertip. These fingertips will be produced by using the Objet 3D printer, which enables their designated fixing to the transducer.

  The **external loading system** will enable loading of the object in all directions of the top hemisphere, with controlled magnitude and velocity of tensile force. The load direction will be achieved by a frame that could be rotated and fixed in all 180° around one of the horizontal axes. A *runner* will be fixed to the frame. A string will then be anchored to the object, inserted through the fixed runner, and attached through a force transducer to a controlled electric piston. This force transducer will measure the loading force, and the controlled the electric piston will enable the control of the force's magnitude and velocity.

3.6. Preliminary Results

Preliminary results of the current stage of work are briefly presented; comprehensive detailed descriptions are introduced in appendix A.

After defining the solution algorithm, the code environment that will support the algorithm and provide its foundations and test bed was written, Appendix A. As described in chapter's 1 prologue, the grasp model code includes: a full spatial grasp dynamic model comprising the grasped object dynamics as well as the dynamics of each link of every finger, and contact model – in order to correlate

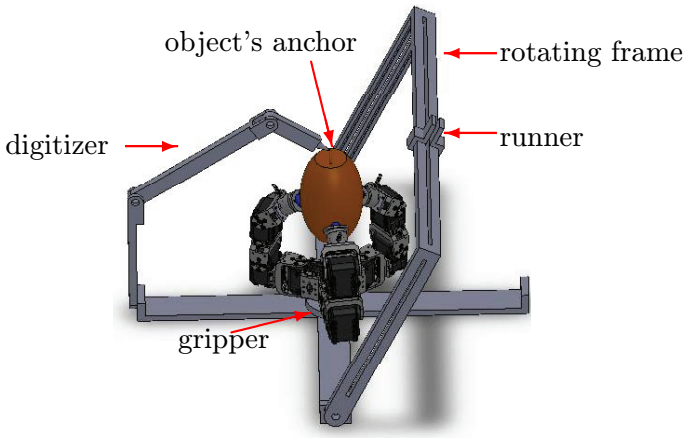

Figure 3.2: Conceptual prototype of the experimental system.

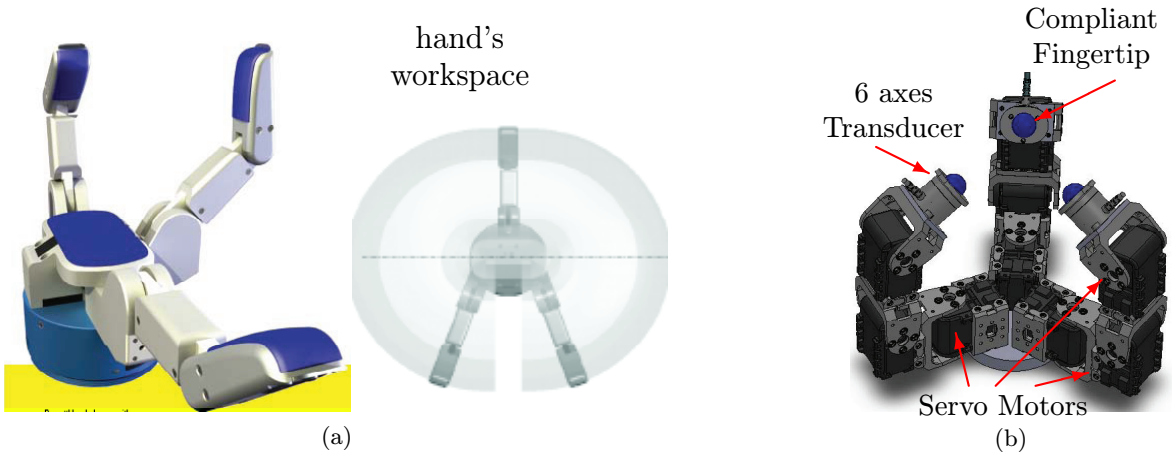

Figure 3.3: Experimental system's hand, based on the Barrett concept. (a) Barrett hand; (b) Experimental system.

the local deformations with the contact points' reactions. The code model further includes a gripper controller that controls the grasped object's position and orientation, and provides initial grasping force.

At this early stage of the work, the simulation code, appendix A, provides:

- ✓ Modular kinematic and dynamic model of the gripper and the object.
- ✓ Modular contact model – can be easily replaced.
- ✓ Solution to the statically indeterminate equations of motion in their equilibrium, based on the mechanical constraints and the first quality criterion – described in section 3.3.
- ✓ Grasp control is performed to the fingertip's position relative to the nominal contact point on the object circumference, as well as to the object's position and orientation.
- ✓ Simulation of the dynamical system's response to an external load.

The following parameters and assumptions are currently considered:

- ☞ The grasped object is an ellipsoid.

Year	2	3		4	
Semester	4	5	6	7	8
Literature review					
Defin contact model					
Gripper controller					
Grasping analysis					
Define the grasp quality criteria					
Grasping synthesis					
Computer simulations					
Building experiments system					
Conducting experiments					
Writing and editing					

Figure 3.4: Research's future progress gant.

- ☞ The gripper has two LLR[3] fingers, with compliant hemisphere fingertips.
- ☞ Tangential friction forces are bounded in the friction cone.
- ☞ The contact model is based on Shapiro et al. [**112**] at the contact points, and it is engaged only after obtaining contact.
- ☞ The contact model considers a small rotational viscosity torque at the contact points – along the normal.
- ☞ Gravity is discarded. In this work it is considered as any other external load.
- ☞ A position and orientation PD grasp controller is used, with no force control.

The simulations provides all of the system's elements' positions and orientations, and the force and torque reactions at the contact points.

The experimental system – as described in section 3.5, is still in construction, Figure 3.2. Further specifications of the system's elements, are studied and refined.

[3]LLR= Linear, Linear, Rotational joints.

APPENDIX A

Preliminary Results - Modeling and Simulations

As mentioned in section 3.6, the programmed code provides an environment where the dynamic system can be simulated, and the grasp model parameters can be calculated and assessed. Its future purpose is to simulate the dynamic behavior of the grasp system, while the optimal grasp solution is implemented. The environment programming is still in progress, therefore this appendix presents two main issues: 1) The current development stage of this environment, and its capabilities. 2) Detailed spatial grasp model, over its variables, indexes and notations.

A full spatial grasp dynamic model comprising the grasped object dynamics as well as the dynamics of each link of every finger and contact model – in order to correlate the local deformations with the contact points' reactions. The code model further includes a gripper controller, whose aims are to control the grasped object's position and orientation, and to provide initial grasping force.

A.1. Kinematic Model

The grasp system (Figure A.1) is constructed of an object that is held by k contact points using a k-finger gripper, assuming the object-gripper contacts are at the gripper's fingertips only. Denote the system's configuration parameters vector to be $\mathbf{q(t)}$. In order to keep the notation short, the time-dependent notation (t) will be neglected, so that

$$\mathbf{q} = (\mathbf{q_0}, \mathbf{q_1}, \ldots, \mathbf{q_k})^T \quad ; \mathbf{q} \in I\!R^{(6+\sum_{i=1}^{k} n_i)}.$$

Define $\mathbf{q_0} \in I\!R^6$ as the object's configuration parameter vector. As a free body it has 6 configuration parameters, notated as $\mathbf{q_0} = (\mathbf{q_{0,1}}, \ldots, \mathbf{q_{0,6}})^T$. The further $\mathbf{q_i} \in I\!R^{n_i}$ where $i = \{1, \ldots, k\}$, are the configuration parameter vectors of the i^{th} gripper's finger. Each finger is modeled as a serial manipulator, constructed of n_i links and the corresponding n_i configuration parameters, so that $\mathbf{q_i} = (\mathbf{q_{i,1}}, \ldots, \mathbf{q_{i,n_i}})^T$.

Denote the inertial frame $W = \{\mathbf{x_0}, \mathbf{y_0}, \mathbf{z_0}\}$. Next, denote $cm_{i,j}$ where $i = \{1, \ldots, k\}, j = \{1, \ldots, n_i\}$ to be the frame, fixed to the j^{th} link of the i^{th} finger, positioned at its center of mass. Using resemble notation, denote $cm_{i,e}$ to be a frame fixed to the i^{th} fingertip. The relative position and orientation of all of $cm_{i,j}$ and $cm_{i,e}$ are performed using an homogeneous transformation, based on the gripper design and the configuration vector $\mathbf{q}$. These transformations define the corresponding rotation matrixes $R_{i,j}, R_{i,e} \in SO(3)$ and the $cm_{i,j}$ and $cm_{i,e}$ origin position vectors $\mathbf{d_{i,j}}, \mathbf{d_{i,e}} \in I\!R^3$. The linear and angular velocities of each $cm_{i,j}$ and $cm_{i,e}$ are calculated using a Jacobian transformation matrix, so that for each link and fingertip

$$\begin{pmatrix} \mathbf{v_{i,j}} \\ \omega_{\mathbf{i,j}} \end{pmatrix} = \begin{bmatrix} Jl_{i,j} \\ J\omega_{i,j} \end{bmatrix} \dot{\mathbf{q}}_\mathbf{i} = J_{i,j}\dot{\mathbf{q}}_\mathbf{i} \quad ; j = \{1, \ldots, n_i, e\}. \tag{A.1}$$

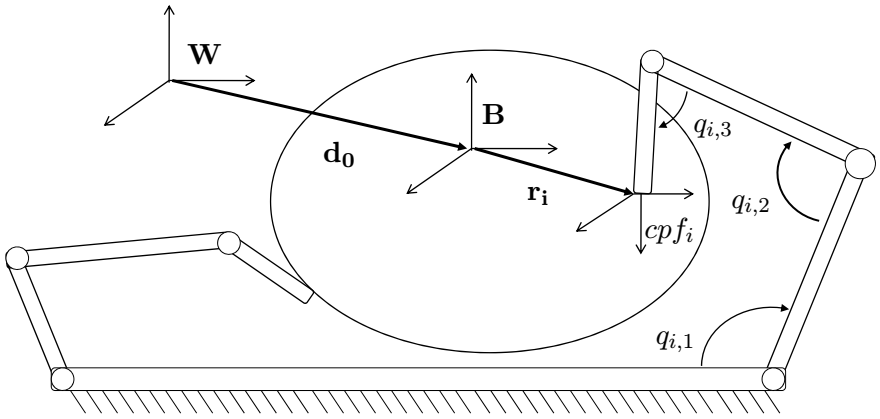

Figure A.1: Schematic kinematic model's parameters.

Denote the object's frame $B = \{\mathbf{x_{obj}}, \mathbf{y_{obj}}, \mathbf{z_{obj}}\}$, oriented and translated relative to W with the corresponding $R_0 \in SO3$ and $d_0 \in I\!R^3$. Each i^{th} contact point is defined on the object's surface relative to B using $\mathbf{r_i}$. It follows that the contact point position in W is

$$\mathbf{cp_i} = R_0\mathbf{r_i} + \mathbf{d_0} = \rho_\mathbf{i} + \mathbf{d_0}.$$

Each contact point further defines a contact point frame cpf_i. It is defined by three orthogonal vectors: $\mathbf{cp_{i,n}}$, the normal to the tangent plane at the contact point – directed inwards in the object, and $\mathbf{cp_{i,t}}, \mathbf{cp_{i,o}}$ belong to the tangent plane, so that $cpf_i = \{\mathbf{cp_{i,n}}, \mathbf{cp_{i,t}}, \mathbf{cp_{i,o}}\}$. Note that cpf_i is given in terms of B; therefore the relative rotation matrix from cpf_i to B is straightforward $R_{B,i} = [\mathbf{cp_{i,n}}|\mathbf{cp_{i,t}}|\mathbf{cp_{i,o}}]$. In order to maintain simplicity, the i^{th} contact point corresponds to the i^{th} finger. Same as (A.1), a Jacobian transformation matrix is used to define cpf_i linear and angular velocities,

$$\begin{pmatrix}\mathbf{v_{0,i}}\\ \omega_\mathbf{0,i}\end{pmatrix} = \begin{bmatrix}Jl_{0,i}\\ J\omega_{0,i}\end{bmatrix}\dot{\mathbf{q}}_\mathbf{0} = J_{0,i}\dot{\mathbf{q}}_\mathbf{0}.$$

A.2. Contact Model

The consideration of friction is based on the rigid body Coulomb friction. This means that the tangential static friction force at the i^{th} contact point $F_{fric,t,i}$ is bounded by the normal reaction force $F_{n,i}$ and the coefficient of friction μ as

$$|F_{fric,t,i}| \leq \mu F_{n,i}. \tag{A.2}$$

The bound in (A.2) is presented in Figure A.2. The relation on the $(F_{fric,t,i}, F_{n,i})$ plane presents an isosceles triangle. The triangles height is $F_{n,i}$, its base corner values are the static tangential friction force bound, and its head vertex is twice the inverse-tangent of μ. The isosceles triangle is a section of the spatial *friction cone*, for the spatial case. Therefore, it is said that there is no slip as long as the reaction forces are "inside" the friction cone, which is equivalent to the fulfillment of (A.2).

The compliant normal and the tangential reaction forces $F_{n,i}, F_{t,i}$ are considered at this stage of research as in Shapiro et al. [**112**]. Considering quasi-rigid spheres with radii R_1, R_2, and identical material properties. Instead of considering the bodies' deformation, the two bodies are considered rigid, while the deformation is modeled as a virtual penetration of the bodies to each other. The reaction

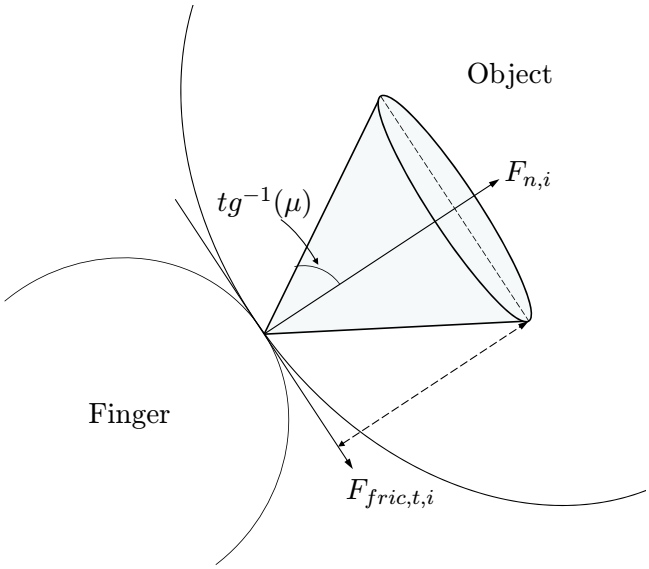

Figure A.2: Schematic friction cone.

forces are a function of these penetrations. The system configuration and, therefore, the virtual penetration depends on the system configuration parameters $\mathbf{q(t)}$. It follows by Johnson [**64**, p.221], that by using the matrix $cpf_i = \left[\mathbf{cp_{i,n}}, \mathbf{cp_{i,t}}, \mathbf{cp_{i,o}}\right]^T$, the normal and the tangential penetrations at the i^{th} contact point are defined as

$$\delta_{\mathbf{i}} = \begin{pmatrix} \delta_{n,i} \\ \delta_{t,i} \\ \delta_{o,i} \end{pmatrix} = \int_0^t cpf_i \left(J_i \dot{\mathbf{q}}_{\mathbf{i}} - J_{0,i} \dot{\mathbf{q}}_{\mathbf{0}}\right) \partial t. \tag{A.3}$$

The normal penetration can be equivalently defined as *the minimal translation of the spheres' centers that would result in the bodies' separation.*

The normal reaction force at the i^{th} contact point $f_{n,i}$ is an outcome of the body's elasticity and viscoelasticity properties of the materials, described by the functions $el_{n,i}(\delta_{n,i}(\mathbf{q}))$ and $vl_{n,i}(\delta_{n,i}(\mathbf{q}), \delta_{t,i}(\mathbf{q}), \delta_{o,i}(\mathbf{q}), \dot{\delta}_{n,i}($
It is of the form:

$$f_{n,i}(\mathbf{q}) = el_{n,i}(\delta_{n,i}(\mathbf{q})) + vl_{n,i}(\delta_{n,i}(\mathbf{q}), \delta_{t,i}(\mathbf{q}), \delta_{o,i}(\mathbf{q}), \dot{\delta}_{n,i}(\mathbf{q})), \tag{A.4}$$

while $el_{n,i}$ and $vl_{n,i}$ are differentiable and further sustain:

$$el_{n,i}(0) = 0 \qquad vl_{n,i}(\delta_{n,i}(\mathbf{q}), \delta_{t,i}(\mathbf{q}), \delta_{o,i}(\mathbf{q}), 0) = 0$$
$$el_{n,i}^{'}(\delta_{n,i}(\mathbf{q})) > 0; \forall \delta_{n,i}(\mathbf{q}) > 0 \qquad vl_{n,i}(\delta_{n,i}(\mathbf{q}), \delta_{t,i}(\mathbf{q}), \delta_{o,i}(\mathbf{q}), \dot{\delta}_{n,i}(\mathbf{q})) \cdot \dot{\delta}_{n,i}(\mathbf{q}) < 0$$

Following Hertz's nonlinear contact model [**53**, p. 146], the viscoelasticity and tangential load are neglected. It follows that (A.3) can be independently performed for the normal direction, so the normal reaction force due to normal compliance is:

$$f_{n,i} = el_{n,i}(\delta_{n,i}(\mathbf{q})) = \frac{8G\sqrt{R}}{3(1-\nu)}(\delta_{n,i})^{3/2}. \tag{A.5}$$

For spheres of different radii, the equivalent radius is $R = \frac{R_1 R_2}{R_1 + R_2}$, an equivalent elastic modulus and shear modulus G are functions of the elastic modulus and Poissons ratio ν, as defined by [**64**, p.92].

The tangential reaction force is too generally based on the materials elasticity and viscoelasticity,

$$\begin{aligned} f_{t,i}(\mathbf{q}) &= el_{t,i}(\delta_{t,i}(\mathbf{q}), \delta_{n,i}(\mathbf{q})) + vl_{t,i}(\delta_{n,i}(\mathbf{q}), \delta_{t,i}(\mathbf{q}), \delta_{o,i}(\mathbf{q}), \dot{\delta}_{n,i}(\mathbf{q})) \\ f_{o,i}(\mathbf{q}) &= el_{o,i}(\delta_{o,i}(\mathbf{q}), \delta_{n,i}(\mathbf{q})) + vl_{o,i}(\delta_{n,i}(\mathbf{q}), \delta_{t,i}(\mathbf{q}), \delta_{o,i}(\mathbf{q}), \dot{\delta}_{n,i}(\mathbf{q})), \end{aligned} \tag{A.6}$$

while $el_{t,i}, el_{o,i}, vl_{t,i}, vl_{o,i}$ are differentiable and further sustain

$$\begin{aligned} &el_{t,i}(\delta_{n,i}(\mathbf{q}), 0) = 0 && vl_{t,i}(\delta_{n,i}(\mathbf{q}), 0, \delta_{o,i}(\mathbf{q}), \dot{\delta}_{t,i}(\mathbf{q})) = 0 \\ &\acute{el}_{t,i}(\delta_{t,i}(\mathbf{q})) > 0; \forall \delta_{t,i}(\mathbf{q}) > 0 && vl_{t,i}(\delta_{n,i}(\mathbf{q}), \delta_{t,i}(\mathbf{q}), \delta_{o,i}(\mathbf{q}), \dot{\delta}_{t,i}(\mathbf{q})) \cdot \dot{\delta}_{t,i}(\mathbf{q}) < 0 \\ &el_{o,i}(\delta_{n,i}(\mathbf{q}), 0) = 0 && vl_{o,i}(\delta_{n,i}(\mathbf{q}), \delta_{t,i}(\mathbf{q}), 0, \dot{\delta}_{t,i}(\mathbf{q})) = 0 \\ &\acute{el}_{o,i}(\delta_{o,i}(\mathbf{q})) > 0; \forall \delta_{o,i}(\mathbf{q}) > 0 && vl_{o,i}(\delta_{n,i}(\mathbf{q}), \delta_{t,i}(\mathbf{q}), \delta_{o,i}(\mathbf{q}), \dot{\delta}_{n,i}(\mathbf{q})) \cdot \dot{\delta}_{o,i}(\mathbf{q}) < 0 \end{aligned}$$

As in Walton [**127, 128**], the tangential reaction forces are defined under the following assumptions: no slip between the bodies, an oblique linear load trajectory of the form $\delta_{t,i} = c_{t,i}\delta_{n,i}$, $\delta_{o,i} = c_{o,i}\delta_{n,i}$ where $c_{t,i}, c_{o,i}$ are scalars, and independency of the two tangential penetrations in each other. It is of the form:

$$\begin{aligned} f_{t,i}(\mathbf{q}) &= el_{t,i}(\delta_{t,i}(\mathbf{q}), \delta_{n,i}(\mathbf{q})) = \frac{16G\sqrt{R}}{3(2-\nu)}\sqrt{\delta_{n,i}}\delta_{t,i} \\ f_{o,i}(\mathbf{q}) &= el_{o,i}(\delta_{o,i}(\mathbf{q}), \delta_{n,i}(\mathbf{q})) = \frac{16G\sqrt{R}}{3(2-\nu)}\sqrt{\delta_{n,i}}\delta_{o,i}. \end{aligned} \tag{A.7}$$

Substituting (A.5) and (A.7) into (A.2), while realizing that for the tangential directions $F_{fric,t,i} = -f_{t,i}$ and $F_{fric,o,i} = -f_{o,i}$ yields the bound of the load trajectory linear's coefficient as $\{|c_{t,i}|, |c_{o,i}|\} \leq \mu\frac{2-\nu}{2(1-\nu)}$.

The reaction torque for the i^{th} contact point T_i has to be defined. At this stage of the research it is discarded and defined generally in (A.8). So the total reaction vector is

$$\tau_{\mathbf{reaction,i}} = \begin{pmatrix} f_i \\ T_i \end{pmatrix}; \mathbf{f_i} = \begin{pmatrix} f_{n,i} \\ f_{t,i} \\ f_{o,i} \end{pmatrix}, \mathbf{T_i} = \begin{pmatrix} T_{n,i} \\ T_{t,i} \\ T_{o,i} \end{pmatrix}. \tag{A.8}$$

The contact model (A.5) and (A.7), does not consider the dissipation of energy due to viscoelasticity and the generation of heat for the case of non-linear load trajectory Elata [**29**]. The object and fingertips' viscoelasticity is modeled as a force proportional to the time derivative of δ_i. In the future of this study, a more detailed and accurate model will be implemented, as described in section 3.2.

A.3. Grasp Control

The gripper's controller aims are two-fold. The first is to grasp the object at the defined contact points, strong enough so it can withstand the load of an external force and torque. The second aim is to position and orient the object as desired. Since grasp control is not the main issue in this work, a simple PD controller is used. The fingertip displacement error is

$$ft_{i,err} = cp_i + (\delta_{pen}cp_{i,n}) - ft_i, \tag{A.9}$$

where δ_{pen} is a nominal desired penetration in the normal to surface direction at the i^{th} contact point. It aims to enforce the controller to apply force to the object. The grasp controller is of the form:

$$\tau_{i,grasp} = Kp_{grasp} \cdot ft_{i,err} + Kd_{grasp} \cdot \dot{ft}_{i,err}, \tag{A.10}$$

where Kp_{grasp}, Kd_{grasp} are positive definite gain matrices. The position and orientation controller uses the error in the contact point present position and its desired position,

$$cp_{i,err} = cp_{i,des} - cp_i. \tag{A.11}$$

The desired position is derived from the object's position and orientation. Therefore, the position and orientation controller is of the form:

$$\tau_{i,pos} = Kp_{pos} \cdot cp_{i,err} + Kd_{pos} \cdot \dot{cp}_{i,err}, \tag{A.12}$$

where Kp_{pos}, Kd_{pos} are positive definite gain matrices. Notice that the objects' orientation can be defined by the control of the appropriately chosen contact points. The overall gripper controller is of the form:

$$\tau_{i,grip} = \tau_{i,grasp} + \begin{cases} \tau_{i,pos} & \text{In contact} \\ 0 & \text{No contact} \end{cases}. \tag{A.13}$$

As seen in (A.13), the position and orientation control is activated only after the fingerobject contact is achieved. Note that the object's position and orientation can be defined by the desired set points of the position controller.

A.4. Dynamic Model

The dynamic equations are constructed using the closed matrix form of the equations of motion, as in Spong [**118**, P.200]. It is built separately for the grasped object and for each finger, and it is of the form:

$$D_i(q_i)\ddot{q}_i + C_i(q_i, \dot{q}_i)\dot{q}_i + G_i(q_i) + fric(\dot{q}_i) = \tau_i, \quad i \in \{0 \dots k\}. \tag{A.14}$$

Here $D_i(q_i)$ is called the *Inertia Matrix*, $C_i(q_i, \dot{q}_i)$ is called the *Coriolis Matrix*, $G_i(q_i)$ is the *gravity vector*, and $fric(\dot{q}_i)$ is an artificially added vector, used to model the viscous friction at the gripper's joints. The external generalized forces vector τ_i, is compound as

$$\tau_i = J_i^T \cdot \begin{pmatrix} F_i \\ T_i \end{pmatrix}, \tag{A.15}$$

where J_i^T is the transpose of the $i^{th'}$ system Jacobian matrix. F_i, T_i are the external force and torque actuated on the system. For $i = 0$, the object's generalized force is given as

$$\tau_0 = \begin{cases} \sum_{i=0}^{k} J_{0,i}^T \cdot \tau_{reaction,i} & \text{In contact} \\ 0 & \text{No contact} \end{cases}, \tag{A.16}$$

and for the $i^{th'}$ finger the generalized force is given as

$$\tau_i = J_i^T \cdot \tau_{i,grip} + \begin{cases} -\sum_{i=0}^{k} J_{0,i}^T \cdot \tau_{reaction,i} & \text{In contact} \\ 0 & \text{No contact} \end{cases}. \tag{A.17}$$

As described for the position and orientation controller, the reaction forces and torques applied to the system only if contact exists.

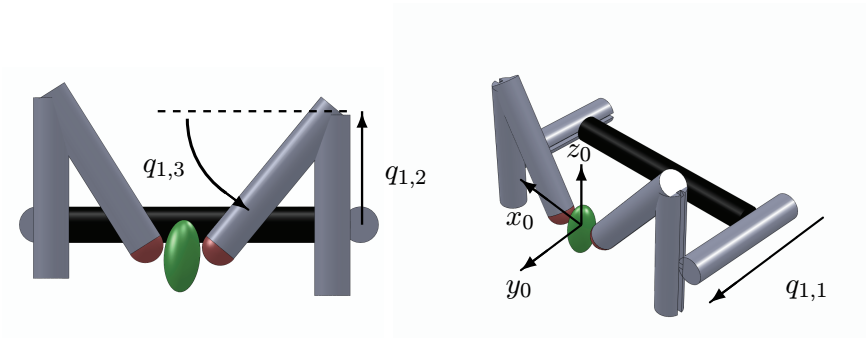

Figure A.3: Simulated gripper and object.

A.5. Simulation Code Result

A numerical simulation is performed in order to demonstrate the constructed system's operation and response. As seen in Figure A.3, the grasped object is an ellipsoid with the major radii $\{50, 70, 100\}[mm]$. The gripper has two fingers, each with three rod shape links and three configuration parameters. The fingers are located on both sides of the ellipsoid along the x_0 axis, and constructed of two linear joints that enable movement parallel to the (y_0, z_0) plane, and a revolving joint whose axis is parallel to (y_0). The initial conditions for the simulation are where the object's center is at $\{0, 0.2, 0.1\}$ and the fingertips are folded down. In that configuration the fingertips do not have contact with the object. The object's desired position is at W's origin. In order to maintain simplicity at these early stages of work, the simulation discards gravity and torque reactions. Other system mechanical properties and controller gains are detailed in Table A.1. The equations are solved in *Wolfram Mathematica* 7^{TM}, using the NDSolve function.

In the simulation, the contact model does not include the torque reactions at the contact point, rather it is considered as zero. Although a small rotational viscosity torque is assumed, it is about the normal at the contact point. The rotational friction model is taken as

$$T_{fric,i,n} = \mu \cdot a_i \cdot \omega_{n,i}. \tag{A.18}$$

where μ is the friction coefficient, a_i is the area of contact, and $\omega_{n,i}$ is the element of the relative angular velocity of the two bodies, in the $\mathbf{cp_{i,n}}$ direction.

A.5.1. Simulation's Results and Analysis. It can be easily seen in Figure A.4(a) that the object is stationary for about one second until it comes in contact with the fingers. The same behavior is seen in Figure A.4(c) and A.4(d) that present the contact reaction forces and the position control forces.

A.5.2. About the simulation code. The code is modular and enables versatility and ease in replacing the system's parameters. High level components such as the number of fingers and links, the contact model, and the gripper's controller can be easily replaced, as well as low level parameters such as links' and object's mechanical properties.

Table A.1: Simulation's parameters

parameter	**magnitude**	**unit**
Link's Length	0.2	[m]
Link's Mass	0.1	[kg]
Object's Mass	1	[kg]
$fric$	0.001	[N·Sec/m],[N·Sec/Rad]
g (gravitation)	0	[m/sec^2]
Kp_{grasp},	diagonal matrix(5,5,5)	[N/m]
Kd_{grasp}	diagonal matrix(1,1,1)	[N·Sec/m]
Kp_{pos}	diagonal matrix(10,10,10)	[N/m]
Kd_{pos}	diagonal matrix(2,2,2)	[N·Sec/m]
ν	0.4	[]
μ	0.01	[N·Sec/Rad·m^2]
G	$0.0006 \cdot 10^9$	[GPa]

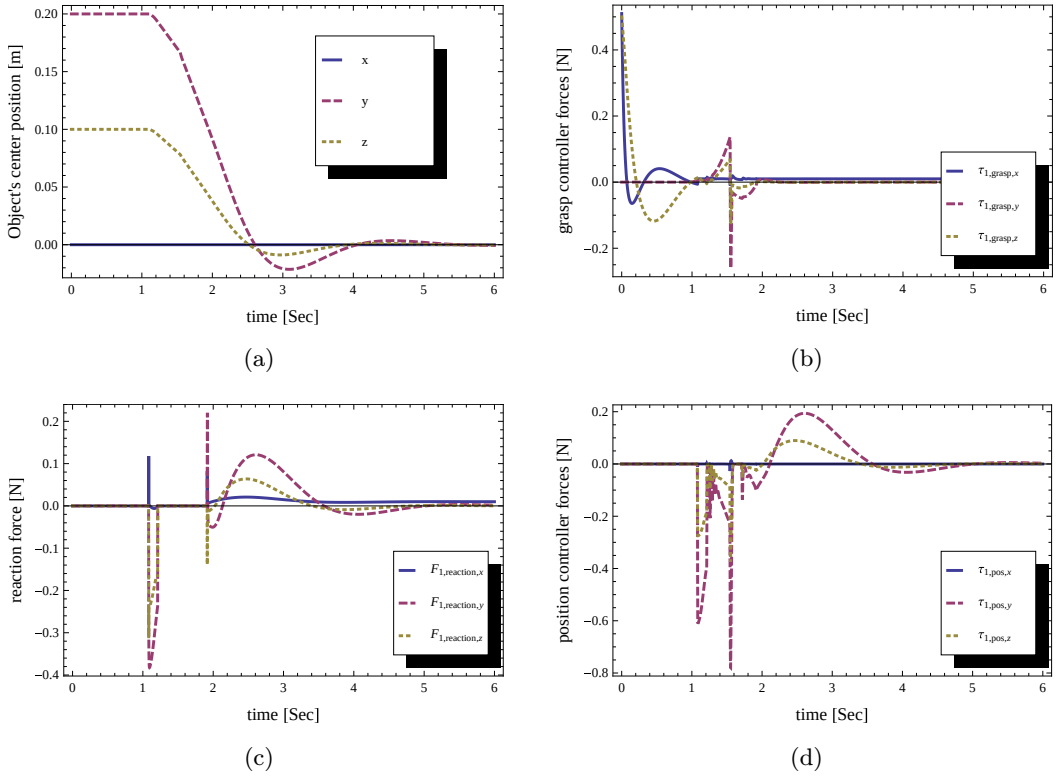

Figure A.4: Simulation results. (a) The object's center position. (b) Grasp control force. (c) Reaction force. (d) Position Control force.

The position and orientation controller, as well as the reaction forces and torques, are applied to the system only after contact is reached. In order to check the existence of contact, the relative position of the fingertip and the nominal contact point is considered. Because *"If"* or *"Step"* functions are not continuous, they may result in a numerical integration error. Smooth continuous differentiable replacement to these functions is

$$step(x) \approx \frac{1}{2}(1 + tanh(ax)), \tag{A.19}$$

where x is the criterion and a is an amplification factor, used to tune the approximation.

Bibliography

[1] ABB-Technologies. Irb 360 flexpicker. http://www.abb.com/, May 2010.

[2] E. Al-Gallaf, A. Allen, and K.vWarwick. a survey of multi-fingered robot hands: issues and grasping achievments. *Mechatronics*, 3(4):465–491, Nov 1993.

[3] P. K. Allen. Graspit!, a robotic grasping simulation tool. http://grasping.cs.columbia.edu, Dec. 2010.

[4] J. A.R., C. R., and P. J.L. A vision system based on a laser range-finder applied to robotic fruit harvesting. *Machine Vision and Applications*, 11(6):321–329, 2000.

[5] ASABE. Compression test of food materials of convex shape. ASABE Standards S368.4, ASABE, 2950 Niles Road, St. Joseph, MI 49085-9659, USA, Dec 2000.

[6] H. Asada and A. By. Kinematic analysis of workpart fixturing for flexible assembly with automatically reconfigurable fixtures. *Journal of Robotics and Automation, IEEE*, 1(2):86 – 94, June 1985.

[7] A. I. Automation. Nano25-e transducer. http://www.ati-ia.com/products/ft/ft_models.aspx?id=Nano25, Feb. 2011.

[8] Barrett-Technology. *Barrett Hand*. Barrett Technology Inc., Barrett Technology, Inc. 625 Mount Auburn Street Cambridge, Massachusetts 02138-4555 USA, 2010. Not In.

[9] M. A. Barrow. Fruit picker. Patent 3397526, USA, Aug 1968.

[10] R. M. Brach. Rigid body collisions. *Journal of Applied Mechanics*, 56(1):133–138, 1989.

[11] R. M. Brach. Formulation of rigid body impact problems using generalized coefficients. *International Journal of Engineering Science*, 36(1):61 – 71, 1998. Not In.

[12] D. Bulanon and T. Kataoka. A fruit detection system and an end effector for robotic harvesting of fuji apples. *Agricultural Engineering International: CIGR Journal*, 12(1):203–210, 2010.

[13] N. Canterakis. 3d zernike moments and zernike affine invariants for 3d image analysis and recognition. In *11th Scandinavian Conference on Image Analysis*, pages 85–93, 1999.

[14] T. Chateau, C. Debain, F. Collange, L. Trassoudaine, and J. Alizon. Automatic guidance of agricultural vehicles using a laser sensor. *Computers and Electronics in Agriculture*, 28(3):243 – 257, 2000.

[15] M. Ciocarlie, C. Goldfeder, and P. Allen. Dimensionality reduction for hand-independent dexterous robotic grasping. In *Proceedings of the IROS, IEEE/RSJ*, pages 3270 –3275, Nov. 2007.

[16] W. P. Coony and S. E. Turner. Fruit picker. Patent 583567, USA, Jun 1897.

[17] G. Coppock. Picking citrus fruit by mechanical means. In *Proceedings Florida State Horticultural Society*, volume 74, pages 247–251, 1961.

[18] W. G. ©. Fruit picker. www.wolf-garten.org, 2009. Article-No.:7242080.

[19] J. D. W. D. B. Churchill, H. R. Sumner. Peel strength properties of three orange varieties. *Transactions of the ASAE*, 23:273–176, 1980.

[20] E. Department of Education and A. Workplace Relations. Crop details,avocados. http://jobsearch.gov.au/HarvestTrail/CropDetails.aspx?CropID=19, Jan. 2011.

[21] R. Diankov, S. Srinivasa, D. Ferguson, and J. Kuffner. Manipulation planning with caging grasps. In *International Conf on Humanoid Robots, IEEE*, 2008.

[22] DIGINFO.TV. Strawberry picking robot. http://www.diginfo.tv/2010/11/30/10-0251-f-en.php, Nov. 30th 2010.

[23] P. Dupont. Friction modeling in dynamic robot simulation. In *Proceedings International Conference on Robotics and Automation-ICRA,IEEE*, volume 2, pages 1370 –1376, May 1990.

[24] P. Dupont. Avoiding stick-slip in position and force control through feedback. In *Proceedings International Conference on Robotics and Automation-ICRA,IEEE*, volume 2, pages 1470 –1475, Apr. 1991.

[25] P. Dupont. The effect of coulomb friction on the existence and uniqueness of the forward dynamics problem. In *Proceedings International Conference on Robotics and Automation-ICRA,IEEE*, volume 2, pages 1442 –1447, May 1992.

[26] P. Dupont. Avoiding stick-slip through pd control. *Transaction on Automatic Control, IEEE*, 39(5):1094 –1097, May 1994.

[27] P. Dupont and S. Yamajako. Jamming and wedging in constrained rigid-body dynamics. In *Proceedings International Conference on Robotics and Automation-ICRA,IEEE*, volume 3, pages 2349 –2354, May 1994.

[28] B. v. T. J. K. J. M. J. B. E.J. van Henten, J. Hemming and E. van Os. An autonomous robot for harvesting cucumbers in greenhouses. *Autonomous Robots*, 13:241–258, 2002.

[29] D. Elata. On the oblique compression of two elastic spheres. *Journal of Applied Mechanics*, 63:1039–1041, 1996.

[30] D. Elata and J. G. Berryman. Contact force-displacement laws and the mechanical behavior of random packs of identical spheres. *Mechanics of Materials*, 24(3):229 – 240, 1996.

[31] F. Erzincanli, J. Sharp, and S. Erhal. Design and operational considerations of a non-contact robotic handling system for non-rigid materials. *International Journal of Machine Tools and Manufacture*, 38(4):353 – 361, 1998.

[32] F. J. Essex E. Random vibration techniques for non-destructive evaluation of peach firmness. *Journal of Agricultural Engineering Research*, 16(1):81 – 87, 1971.

[33] J. Essex E., Finney. Dynamic elastic properties and sensory of apples fruit. *Journal of Texture Studies*, 2(1):62–74, Jan 1971.

[34] T. Feix, R. Pawlik, H. Schmiedmayer, J. Romero, and D. Kragic. A comprehensive grasp taxonomy. In *Robotics, Science and Systems Conference: Workshop on Understanding the Human Hand for Advancing Robotic Manipulation*, 2009.

[35] T. Feix, R. Pawlik, H.-B. Schmiedmayer, J. Romero, and D. Kragic'. Human grasping database, http://web.student.tuwien.ac.at/~e0227312/. http://web.student.tuwien.ac.at/ e0227312/, Dec 2010.

[36] Festo. *Modular Lightweight Adaptive Gripper with "FinRay-Effect"* ©, Apr 2010.

[37] E. Finney. Dynamic elastic properties of some fruits during growth and development. *Journal of Agricultural Engineering Research*, 12(4):249 – 256, 1967.

[38] W. Friedrich, P. Lim, and H. Nicholl. Sensory gripping system for variable products. In *Proceedings International Conference on Robotics and Automation-ICRA,IEEE*, volume 2, pages 1982 –1987 vol.2, 2000.

[39] S. Futch and F. Roka. Continuous canopy shake mechanical harvesting systems. *EDIS. UF/IFAS. FL*, 2005.

[40] K. Goldberg and K. Gopalakrishnan. D-space and deform closure: a framework for holding deformable parts. In *Proceedings International Conference on Robotics and Automation-ICRA,IEEE*, volume 1, pages 345–350, 2004.

[41] C. Goldfeder. *Data-Driven Grasping*. PhD thesis, Columbia University, 2010.

[42] C. Goldfeder, P. Allen, C. Lackner, and R. Pelossof. Grasp planning via decomposition trees. In *Proceedings International Conference on Robotics and Automation-ICRA,IEEE*, pages 4679 –4684, 2007.

[43] C. Goldfeder, M. Ciocarlie, H. Dang, and P. Allen. The columbia grasp database. In *Proceedings International Conference on Robotics and Automation-ICRA,IEEE*, pages 1710 –1716, May 2009.

[44] S. H., K. G., Y. I., and I. T. Robotic harvesting system for eggplants. *Japan Agricultural Research Quarterly (JARQ)*, 63(3):163–168, 2002.

[45] J. D. B. H. Chen. Finite-element-based modal analysis of fruit firmness. *Transactions of the ASAE*, 36(6)(0001-2351):1827–1833, 1993.

[46] J. D. B. H. Chen. Modal analysis of the dynamic behavior of pineapples and its relation to fruit firmness. *Transactions of the ASAE*, 36(5)(92-6511.):1439–1444, 1993.

[47] V. B. H. Chen, J. De Baerdemaeker. Finite element study of the melon for nondestructive sensing of firmness. *Transactions of the ASAE*, 39(3):1057–1065, 93-6599 1996.

[48] I. Han and B. J. Gilmore. Multi-body impact motion with friction—analysis, simulation, and experimental validation. *Journal of Mechanical Design*, 115(3):412–422, 1993.

[49] R. Harrell, P. Adsit, and D. Slaughter. Real time vision servoing of a robotic tree fruit harvester. *ASAE Winter Meeting*, (85–3550), 12 1985.

[50] J. Heilala, T. Ropponen, and M. Airila. Mechatronic design for industrial grippers. *Mechatronics*, 2(3):239 – 255, 1992. Special Issue Mechatronics-a Key Competence in Finland.

[51] J. Hemming, W. Bac, and B. van Tuijl. Workpackage 5: Sweet pepper - protected cultivation, deliverable 5.1. Technical report, Wageningen University and Research Centre(WUR). Netherlands, Jan. 2011. Design objectives and requirements for a sweet pepper harvesting robot (Deliverable 5.1) in the framework of the Crops EU project.

[52] H. Hertz. On the contact of elastic solids [german]. *Journal reine angew. Math*, 92:156–171, 1881.

[53] H. Hertz. *Hertz Miscellaneous Papers*. Macmillan and Co., 1896. translated from German to English by D. E. Jones, and G. A. Schott.

[54] M. Hilaga, Y. Shinagawa, T. Kohmura, and T. L. Kunii. Topology matching for fully automatic similarity estimation of 3d shapes. In *Proceedings of the 28th annual Conference on Computer graphics and interactive techniques*, SIGGRAPH '01, pages 203–212, New York, NY, USA, 2001. ACM.

[55] M. K. Ho Choi. Design and feasibility tests of a flexible gripper based on inflatable rubber pockets. *International Journal of Machine Tools & Manufacture*, 46:1350–1361, Oct 2006.

[56] R. Howe, I. Kao, and M. Cutkosky. The sliding of robot fingers under combined torsion and shear loading. In *Proceedings International Conference on Robotics and Automation-ICRA,IEEE*, volume 1, pages 103 –105, Apr. 1988.

[57] R. D. Howe and M. R. Cutkosky. Practical force-motion models for sliding manipulation. *The International Journal of Robotics Research-IJRR*, 15(6):557–572, 1996.

[58] D. R. I. Shmulevich, N. Galili. Detection of fruit firmness by frequency analysis. *Transactions of the ASAE*, 39(3)(93-6027):1047–1055, 1996.

[59] L. Ingber. Very fast simulated re-annealing. *Mathematical and Computer Modelling*, 12(8):967 – 973, 1989.

[60] R. L. J. A. Abbott. Anisotropic mechanical properties of apples. *Transactions of the ASAE*, 39(4)(94-6604):1451–1459, 1996.

[61] V. M. J. Felfoldi. Finite element method for interpretation of sample vibrations. *ASAE Annual International Meeting*, (056174):1–11, Jul 2005.

[62] K. Jamshidi. Fruits and nuts picking device. Patent 3664104, USA, 124-4th Avenue N.W. Faribault Minn. 55021, March 1972.

[63] K. L. Johnson. Surface interaction between elastically loaded bodies under tangential forces. *Proceedings of the Royal Society of London. Series A, Mathematical and Physical Sciences*, 230(1183):531–548, July 1955.

[64] K. L. Johnson. *Contact Mechanics*. Cambridge University Press, 1985. ISBN 0 521 34796 3.

[65] S. Johnson and S. H.Bowman. Fruit picker. Patent 556822, USA, Oct 1944.

[66] G. S. Jörg Stephan. Handling with ice the cryo-gripper, a new approach. *Journal of Assembly Automation*, 19(4):332–337, 1999.

[67] I. Kamon, T. Flash, and S. Edelman. Learning visually guided grasping: a test case in sensorimotor learning. *Transactions on Systems, Man and Cybernetics, Part A: Systems and Humans, IEEE*, 28(3):266 –276, May 1998.

[68] J. B. Keller. Impact with friction. *Journal of Applied Mechanics*, 53(1):1–4, 1986.

[69] C. F. Kellogg. Fruit picker. Patent 301915, USA, Aug 1915.

[70] G. L. and J. W.Brown. Fruit picker. Patent 914502, USA, Mar 1901.

[71] G. Leifman, S. Katz, A. Tal, and R. Meir. Signatures of 3d models for retrieval, 2003.

[72] D. H. Lenker. Development of an auger picking head for selectively harvesting fresh market oranges. *Transactions of the ASAE.*, 13(4):500–507, 1970.

[73] D. H. Lenker and S. Hedden. Limb properties of citrus as criteria for tree-shaker design. *Transactions of the ASAE.*, 11(1):129–135, 1968.

[74] L.H.Swift. Fruit picker head. Patent 3552107, USA, 1971.

[75] Q. Lin, J. Burdick, and E. Rimon. A stiffness-based quality measure for compliant grasps and fixtures. *Transactions on Robotics and Automation, IEEE*, 16(6):675 –688, dec 2000.

[76] P. Ling, R. Ehsani, K. Ting, Y. Chi, N. Ramalingam, M. Klingman, and C. Draper. Sensing and end-effector for a robotic tomato harvester. *ASAE Annual Meeting*, (043088), 8 2004.

[77] K. H. Y. E. M. Cardenas Weber, R. L. Stroshine. Melon material properties and finit element analysis of melon compresson with application to robot gripping. *Transactions of the ASABE.*, 34(3)(0001-2351):920–929, 1991.

[78] E. O. A. S. M. Marco Ceccarelli, Giorgio Figliolini and E. J. Criado. Designing a robotic gripper for harvesting horticulture products. *Robotica*, 18(1):105–111, 2000.

[79] A. Miller and P. Allen. Graspit! a versatile simulator for robotic grasping. *Robotics Automation Magazine, IEEE*, 11(4):110 – 122, 2004.

[80] A. Miller, S. Knoop, H. Christensen, and P. Allen. Automatic grasp planning using shape primitives. In *Proceedings International Conference on Robotics and Automation-ICRA,IEEE*, volume 2, pages 1824 – 1829 vol.2, 2003.

[81] R. D. Mindlin. Compliance of elastic bodies in contact. *ASME-J. of Applied Mechanics*, 16:259–268, 1949.

[82] B. E. R. N., A. J., M. A., S. E., Z. M., L. H., and J. H. Universal robotic gripper based on the jamming of granular material. In D. Meiron, editor, *Proceedings of the National Academy of Sciences*, volume 107, pages 18809–18814, 2010.

[83] N. B. N. Galili, I. Shmulevich. Acoustic testing of avocado for fruit ripness evaluation. *Transactions of the ASABE.*, 41(2)(0001-2351):399–407, 1998.

[84] M. Novotni and R. Klein. 3d zernike descriptors for content based shape retrieval. In *Proceedings of the eighth ACM symposium on Solid modeling and applications*, SM '03, pages 216–225, New York, NY, USA, 2003. ACM.

[85] Y. Or. *Frictional equilibrium postures for robotic locomotion - computation, geometric characterization, and stability analysis*. PhD thesis, The Technion - ISRAEL Institute of Tecnology, May 2007.

[86] Y. Or and E. Rimon. Robust multiple contact postures in a two-dimensional gravitational field. In *Proceedings International Conference on Robotics and Automation-ICRA,IEEE*, volume 5, pages 4783 – 4788, May 2004.

[87] Y. Or and E. Rimon. Computation and graphical characterization of robust multiple-contact postures in 2d gravitational environments. In *Proceedings International Conference on Robotics and Automation-ICRA,IEEE*, pages 247 – 252, 2005.

[88] Y. Or and E. Rimon. On the hybrid dynamics of planar mechanisms supported by frictional contacts. i: necessary conditions for stability. In *Proceedings International Conference on Robotics and Automation-ICRA,IEEE*, pages 1213 –1218, May 2008.

[89] R. Osada, T. Funkhouser, B. Chazelle, and D. Dobkin. Shape distributions. *ACM Transactions Graph.*, 21:807–832, 2002.

[90] R. Pelossof, A. Miller, P. Allen, and T. Jebara. An svm learning approach to robotic grasping. In *Proceedings International Conference on Robotics and Automation-ICRA,IEEE*, volume 4, pages 3512 – 3518, May 2004.

[91] A. Pettersson, S. Davis, J. Gray, T. Dodd, and T. Ohlsson. Design of a magnetorheological robot gripper for handling of delicate food products with varying shapes. *Journal of Food Engineering*, 98:332–338, 2010.

[92] J. H. Piater and J. H. Piater. Learning visual features to recommend grasp configurations. Technical report, University of Massachusetts, 2000.

[93] D. C. P.Y. Chua, T. Ilschner. Robotic manipulation of food products - a review. *International Journal of Industrial Robot*, 30:345–354, 2003.

[94] C. R., P. J.L., J. A.R., M. J.M., and C. L. Design and implementation of an aided fruit-harvesting robot (agribot). *InternationalJournal of Industrial Robot*, 25(5):337–346, 1998.

[95] J. N. Reed, S. J. Miles, J. Butler, M. Baldwin, and R. Noble. Ae–automation and emerging technologies: Automatic mushroom harvester development. *Journal of Agricultural Engineering Research*, 78(1):15 – 23, 2001.

[96] E. Rimon and J. Burdick. Mobility of bodies in contact. i. a new 2nd order mobility index for multiple-finger grasps. In *Proceedings International Conference on Robotics and Automation-ICRA,IEEE*, volume 3, pages 2329 –2335, Aug 1994.

[97] E. Rimon and J. Burdick. Mobility of bodies in contact. ii. how forces are generated by curvature effects? In *Proceedings International Conference on Robotics and Automation-ICRA,IEEE*, volume 3, pages 2336 –2341, May 1994.

[98] E. Rimon and J. Burdick. A configuration space analysis of bodies in contact–ii. 2nd order mobility. *Mechanism and machine theory*, 30(6):913–928, 1995.

[99] E. Rimon and J. W. Burdick. A configuration space analysis of bodies in contact–i. 1st order mobility. *Mechanism and Machine Theory*, 30(6):897 – 912, 1995.

[100] ROBOTIS. Dynamixel ax-12+. http://www.robotis.com/xe/dynamixel_en, Feb. 2011.

[101] B. Rössler and J. Zhang. Visual guided grasping of aggregates using self-valuing learning. In *Proceedings International Conference on Robotics and Automation-ICRA,IEEE*, volume 4, pages 3912–3917, 2002.

[102] E. J. Routh. *Dynamics of a System of Rigid Bodies*. Macmillan and Co., 7 edition, 1905.

[103] B. P. V. D. S. N. S. E. Prussia, M. K. Tetteh. Apparent modulue of elasticity from firmtech2 firmness measurements of brlueberries. *Transactions of the ASABE*, 49(1):113–121, 2006.

[104] A. A. T. S. J. Flood, T. F. Burks. Physical properties of oranges in response to applied gripping forces for robotic harvesting. *Transactions of the ASABE.*, 49(2)(061142):341–346, Jul 2006.

[105] S. Sakai, M. Iida, and M. Umeda. Heavy material handling manipulator for agricultural robot. In *Proceedings International Conference on Robotics and Automation-ICRA,IEEE*, volume 1, pages 1062 – 1068, 2002.

[106] S. Sakai, K. Osuka, and M. Umeda. Use of a heavy material handling agricultural robot for harvesting watermelons. In *Proceedings of the International Conference on Automation technology for off-road equipment.*, number 701P1004, pages 321–331. Amer Society of Agricultural, 2004.

[107] R. Sam and S. Nefti. Design and development of flexible robotic gripper for handling food products. In *Intl. Conference on Control, Automation, Robotics and Vision*, pages 17–20. IEEE, Dec 2008.

[108] M. Santello, M. Flanders, and J. F. Soechting. Postural hand synergies for tool use. *Journal Neurosci.*, 18(23):10105–10115, 1998.

[109] A. Shapiro. *Design and Control of an Autononous Spider-Like Robot for Motion in 2D Tunnels Environments*. PhD thesis, the Technion - IRSREAL Institute of Technology, Oct 2003.

[110] A. Shapiro, A. Greenfield, and H. Choset. Frictional compliance model development and experiments for snake robot climbing. In *Proceedings International Conference on Robotics and Automation-ICRA,IEEE*, pages 574 –579, 2007.

[111] A. Shapiro, E. Rimon, and J. Burdick. Passive force closure and its computation in compliant-rigid grasps. In *Proceedings of the International Conference on IROS, IEEE/RSJ*, volume 3, 2001.

[112] A. Shapiro, E. Rimon, and J. W. Burdick. On the mechanichal of natural compliance in frictional contacts and its effect on grasp stiffness and stability. 2010.

[113] P. Shilane, P. Min, M. Kazhdan, and T. Funkhouser. The princeton shape benchmark. In *Proceedings of Shape Modeling International (SMI04)*, pages 167 – 178, 2004.

[114] A. Shpiro, E. Rimon, and S. Shoval. On the passive force closure set of planar grasps and fixtures. *The International Journal of Robotics Research-IJRR*, 29(11):1435–1454, Sep 2010.

[115] W. Simonton. Physical properties of zonal geranium cuttings. *Transactions of the ASABE.*, 35(6)(0001-2351):1899–1904, Aug. 1992.

[116] P. Sinha and J. Abel. A contact stress model for multifingered grasps of rough objects. *Transactions on Robotics and Automation. IEEE*, 8(1):7 –22, Feb. 1992.

[117] B. Sonnenberg. Cucumber harvester. Patent 4,553,381, USA, Waterford, Ontario, Canada N0E 1Y0, 1985.

[118] M. W. Spong, S. Hutchinson, and M. Vidyasagar. *Robot Modeling And Control*. John Wiley &Sons,Inc., 2006.

[119] G. Stellin, G. Cappiello, S. Roccella, M. Carrozza, P. Dario, G. Metta, G. Sandini, and F. Becchi. Preliminary design of an anthropomorphic dexterous hand for a 2-years-old humanoid: towards cognition. In *International Conference on Biomedical Robotics and Biomechatronics, IEEE/RAS-EMBS*, pages 290–295. IEEE, 2006.

[120] W. J. Stronge. Rigid body collisions with friction. In *Proceedings of Mathematical and Physical Sciences*, volume 431, pages 169–181. The Royal Society, Oct. 1990.

[121] W. Townsend and J. Salisbury, J. The effect of coulomb friction and stiction on force control. In *Proceedings International Conference on Robotics and Automation-ICRA,IEEE*, volume 4, pages 883 – 889, Mar. 1987.

[122] C.-H. D. Tsai, I. Kao, A. Shibata, K. Yoshimoto, M. Higashimori, and M. Kaneko. Experimental study of creep response of viscoelastic contact interface under force control. In *IROS, IEEE/RSJ*, pages 4275 –4280, 2010.

[123] J. Ueda, A. Ikeda, and T. Ogasawara. Grip-force control of an elastic object by vision-based slip-margin feedback during the incipient slip. *Transactions on Robotics, IEEE*, 21(6):1139–1147, 2005.

[124] M. Vahedi and A. F. van der Stappe. Caging polygons with two and three fingers. *The International Journal of Robotics Research-IJRR*, 27:1308–1324, Nov./Dec. 2008.

[125] J. D. W. W. M. Miller, J. K. Burns. Effect of harvesting practics on damage to florida grapefruit and oranges. *Journal Applied Engineering in Agriculture.*, 11(2)(93-6502):256–269, Sept 1994.

[126] P. J. Wallin. Robotics in the food industry: an update. *Trends in Food Science & Technology*, 8(6):193 – 198, 1997.

[127] K. Walton. The oblique compression of two elastic shperes. *Journal Mech. Phys. Solids*, 26:139–150, 1978.

[128] K. Walton. The effective elastic moduli of a random packing of spheres. *Journal Mech. Phys. Solids*, 35(2):213–226, 1987.

[129] Y. Wang, V. Kumar, and J. Abel. Dynamics of rigid bodies undergoing multiple frictional contacts. In *Proceedings International Conference on Robotics and Automation-ICRA,IEEE*, pages 2764 –2769 vol.3, May 1992.

[130] Y. Wang and M. T. Mason. Two-dimensional rigid-body collisions with friction. *Journal of Applied Mechanics*, 59(3):635–642, 1992.

[131] J. Whitney. A review of citrus harvesting in florida. In *Transactions Citrus Eng. Conf*, volume 41, pages 33–60, 1995.

[132] J. D. Whitney. Performence of tree air shaker patterns in citrus. *Transactions of the ASAE.*, 21(3):435–441, 1978.

[133] J. D. Whitney. History of mechanical harvesting in florida citrus. http://citrusmh.ifas.ufl.edu/index.asp?p=0&s=11, 6 2006. http://citrusmh.ifas.ufl.edu/images/history/010.jpg.

[134] J. D. Whitney and J. M. Patterson. Development of a citrus removal device using oscilating forced air. *Transactions of the ASAE.*, 15(5):849–860, 1972.

[135] J. D. Whitney, H. R. Sumner, and S. Hedden. Foliage shaker for citrus harvesting - part 2: Harvesting. *Transactions of the ASAE.*, 18(1):70–73, 1975.

[136] C. Xiong, M. Wang, Y. Tang, and Y. Xiong. Compliant grasping with passive forces. *Journal of Robotic Systems*, 22(5):271–285, 2005.

[137] C.-H. Xiong, Y.-F. Li, H. Ding, and Y.-L. Xiong. On the dynamic stability of grasping. *The International Journal of Robotics Research-IJRR*, 18:951–958, 1999.

[138] N. Xydas, M. Bhagavat, and I. Kao. Study of soft-finger contact mechanics using finite elements analysis and experiments. In *Proceedings International Conference on Robotics and Automation-ICRA,IEEE*, volume 3, pages 2179 –2184, 2000.

[139] N. Xydas and I. Kao. Modeling of contact mechanics and friction limit surfaces for soft fingers in robotics, with experimental results. *The International Journal of Robotics Research-IJRR*, 18(8):941–950, 1999.

[140] T. Yoshikawa. Passive and active closures by constraining mechanisms. In *Proceedings International Conference on Robotics and Automation-ICRA,IEEE*, volume 2, pages 1477 –1484, Apr 1996.

[141] Y.Sarig. Robotics of fruit harvesting: A state-of-the-art review. *Journal of Agricalture Engineering Ressurch*, (54):265–280, 1993.

[142] T. Zaharia and F. Prêteux. Header for spie use 3d shape-based retrieval within the mpeg-7 framework. In *Proceedings SPIE Conference on Nonlinear Image and Pattern Analysis XII,*, volume 4304, page 133145. Citeseer, Jan. 2001.

[143] T. Zaharia and F. Preteux. Shape-based retrieval of 3d mesh models. In *Proceedings Inter. Conference on Multimedia and Expo-ICME. IEEE*, volume 1, pages 437 – 440, 2002.